TABLE 2. *V3 loop sequences of clade B HIV-1 strains*

HIV-1 strain	Tropism	V3 loop sequence
MN	X4	CTRPNYNKRKRIHIGPGRAFYTTKNIKGTIRQAHC
BaL	R5	-----N-T--S--------L---GE-I-D------
JR-FL	R5	-----N-T--S------------GE-I-D------

Dashes indicate identical amino acid residue.

DISCUSSION

The V3 loop of HIV-1 gp120 is flexible and structurally diverse, as evidenced by the wide range of different conformations of Arg^{315} observed in gp120 and Fab/V3 complexes (aligned GPGR arches shown in **Fig. 4*A***). This diverse loop, and specifically Arg^{315}, which correlates with genotypic specificity, is also recognized in a variety of ways by anti-V3 mAbs. Although most mAbs interact with their respective antigen through heavy chain interactions (68), several anti-V3 mAbs interact with Arg^{315} through residues of their light chains. For example, murine Fab 83.1 interacts with Arg^{315} through hydrogen bond between the main and side chains of Thr^{L91} (55) (Fig. 4*B*). Human Fab 2219 recognizes Arg^{315} through a hydrogen bond with Asn^{L31} (69) (Fig. 4*C*). In the human F425-B4e8 Fab/V3 complex, Arg^{315} is sandwiched between residues Tyr^{L32} and Asp^{L92} and is stabilized by a salt bridge with Asp^{L92}, as well as hydrogen bonds with the main and side chains of Asp^{L92} (58) (Fig. 4*D*). Additionally, Arg^{315} interacts with the human 1006-15D Fab through hydrogen bonds with the side chains of Asn^{L30} and Asp^{L93} (60) (Fig. 4*E*). KD-247 also uses its light chain to recognize Arg^{315}, but in what appears to be a different manner than other anti-V3 mAbs: in addition to hydrogen bond interactions with Tyr^{L92} and van der Waals interactions with Tyr^{L32} and Tyr^{L92}, Asn^{L27d} also forms a hydrogen bond with the Arg^{315} side chain, providing additional stability. Asn^{L27d} and Tyr^{L32} are held in place by an elaborate hydrogen bond network also involving Asp^{L28} (Fig. 2*D*). These distinct interactions involve the unique CDR L1 insertion of KD-247 and provide a plausible answer for why Arg^{315} is needed for HIV-1 neutralization by KD-247.

The interactions between mAbs and the V3 loop are also affected by the use of different CDRs. For example, the human mAb 537-10D recognizes the same IGPGR epitope as KD-247, yet it uses a long insertion in the CDR H3 loop to make nonspecific interactions with the V3 loop in the form of a 4-stranded antiparallel β-sheet (**Fig. 5*A***), in comparison to KD-247, which primarily uses CDR L1 for V3 loop interactions (Fig. 5*B*, *C*). Although they recognize the same epitope, 537-10D demonstrates a narrow HIV-1 neutralization profile

TABLE 3. *Fifty percent neutralization concentration (EC_{50}) (μM) against clade B HIV-1*

Assay	HIV-1_{MN}(CXCR4-tropic)	HIV-1_{BaL}(CCR5-tropic)
Maraviroc	>0.1	0.002 ± 0.001
KD-247 Fab	0.2 ± 0.06	0.1 ± 0.02
KD-247 scFv	0.7 ± 0.2	0.6 ± 0.1
N27dD scFv	2.1 ± 0.7	1.2 ± 0.2
Y92F scFv	0.8 ± 0.08	0.5 ± 0.09

Data represent the mean ± SD from the results of three independent experiments.

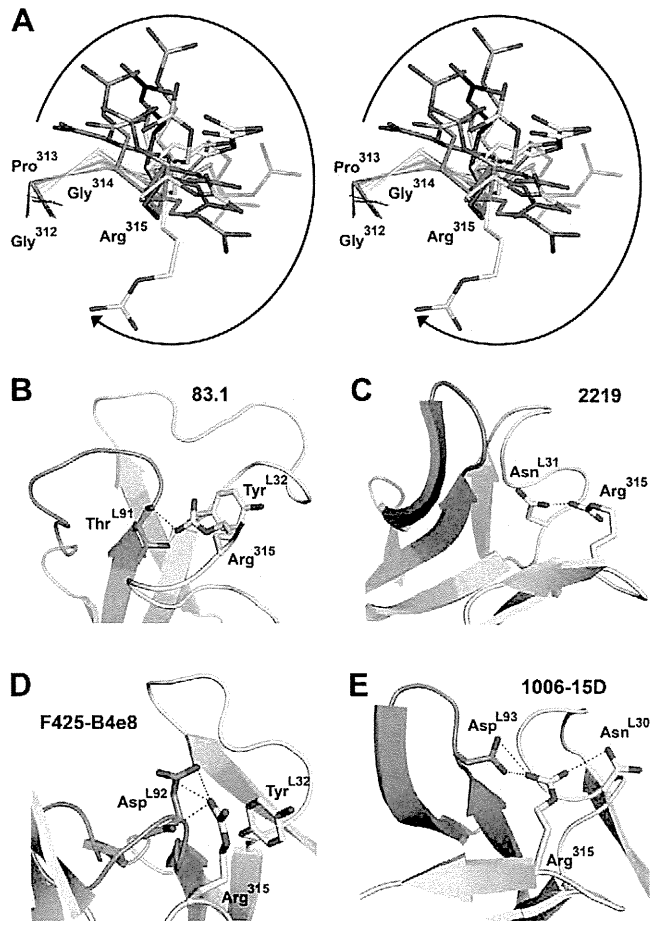

Figure 4. Structural variability of Arg^{315} and recognition by anti-V3 mAb light chains. (A) Stereo view of "GPGR"-containing V3 loops in the following: 58.2 Fab complexes (PDB ID: 1F58, red; 2F58, green; 3F58, magenta), 83.1 Fab complex (1NAK, yellow); 447-52D (1Q1J, orange); 2219 Fab complex (2B0S, pink); F425-B4e8 Fab complex (2QSC, dark gray); 268-D Fab complex (3GO1, gray); 1006-15D Fab complex (3MLW, brown); 3074 Fab complex (3MLX, blue); 2557 Fab complexes (3MLR, light green; 3MLT, cyan); 2558 Fab complex (3UJI, mauve); 537-10D Fab complex (3GHE, hot pink); the V3 loop from the X5 Ab complex with JR-FL gp120 and CD4 (2B4C, dark green); and the V3 loop from the sulfated-tyrosine 412d Ab complex with YU2 gp120 and CD4 (2QAD, light blue). Arrow indicates the space occupied by Arg^{315} conformations in the various structures. Arg^{315} is also stabilized by interactions with light chain residues in some mAbs, including 83.1 (B), 2219 (C), F425-B4e8 (D), and 1006-15D (E). H bonds and salt bridges are shown as black and red dashed lines.

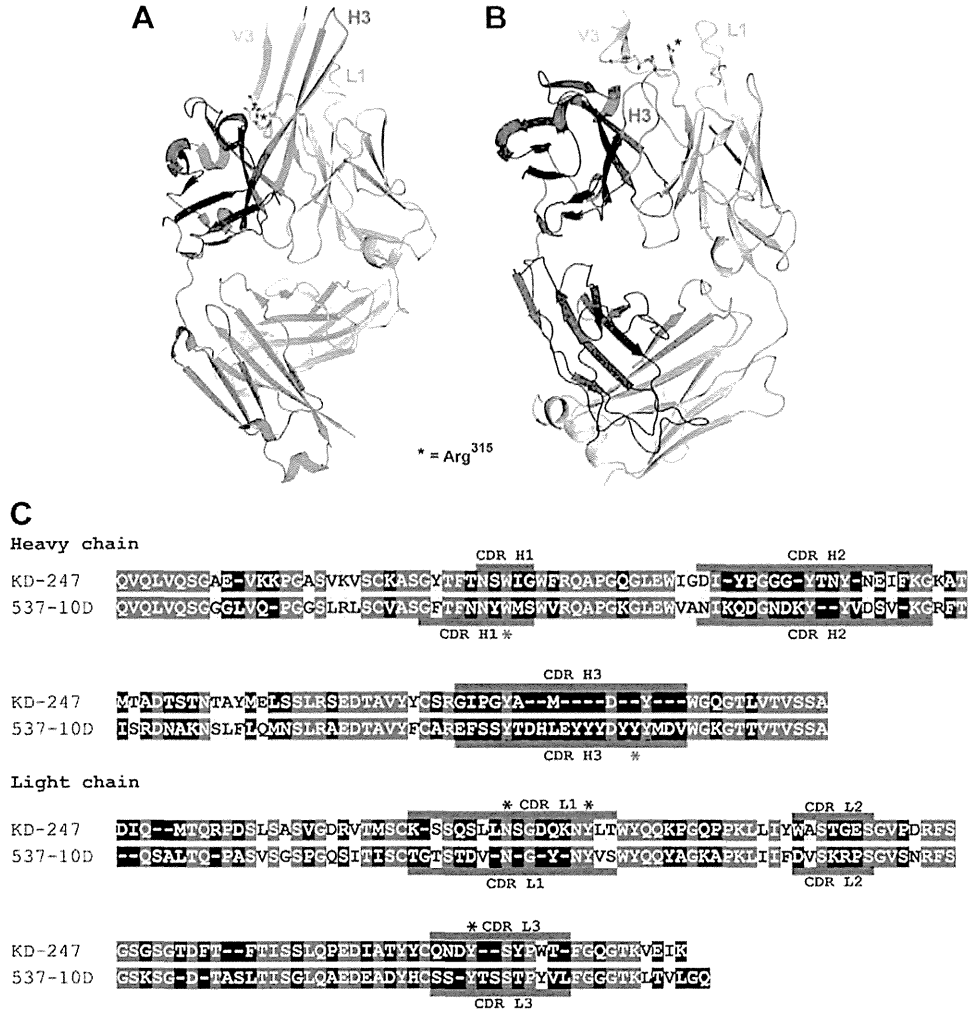

Figure 5. The 537-10D and KD-247 target the same IGPGR epitope using different modes of V3 binding. (A) 537-10D Fab (heavy and light chains in dark and light gray) in complex with an MN V3 peptide (yellow, PDB ID: 3GHE). The primary binding interactions occur in the CDR H3 loop (purple). (B) KD-247 Fab bound to the RP142 V3 peptide (same colors as in (A)). Most of the binding interactions occur in the CDR L1 loop (cyan). (C) Sequence alignment of the KD-247 and 537-10D variable regions (CDR regions in red). Identical residues are highlighted in blue and similar residues in yellow. Asterisks mark the residues making interactions with Arg^{315} of the RP142 V3 peptide. Sequence alignment was performed by the Sequence Manipulation Suite (*http://www.bioinformatics.org/sms2/index.html*). CDRs were labeled on the basis of previously published sequences (27, 59).

compared to KD-247 (70). This is likely due in part to the more restricted antigen binding site of 537-10D, in which the Trp^{H33}, Glu^{H95}, and Tyr^{H100J} residues that interact with Arg^{315} of the V3 loop are buried in a deep pocket (~6Å) that requires a close fit to bind the V3 loop. The CDR region of KD-247 demonstrates a shallow binding pocket that may be able to better tolerate flexibility of the V3 arch (59).

Resistance mutations at gp120 affect interactions between mAb and V3 loop and help HIV-1 escape neutralizing antibodies. Two mutations in the V3 arch region of gp120 cause resistance to KD-247. KD-247 neutralizes $HIV\text{-}1_{JR\text{-}FL}$ with a G314E mutation ~20-fold less efficiently than WT (62), and also binds 100× weaker than WT to $HIV\text{-}1_{BaL}$ with a V2 PNGS insertion in addition to the V3 R315K mutation (63). Our modeling studies suggest that mutation from Gly to Glu at 314 and from Arg to Lys at 315 creates steric interactions with the binding pocket of KD-247 (data not shown). These steric contacts likely affect KD-247 binding to V3 loops containing these mutations and may explain the reported differences in KD-247 binding and HIV-1 neutralization.

Our proposed interactions were validated by the generated scFv variants and the results of our binding and neutralization assays. The data suggest that KD-247 uses an elaborate network of interactions that are based on the long insertion in CDR L1 and involve residues Asn^{L27d}, Asp^{L28}, Tyr^{L32}, and Tyr^{L92} (Fig. 2*D*). Importantly, one of these residues (Tyr^{L32}) appears to be important for proper scFv folding, as almost all of the mutants at this position were inactive in neutralization assays (Fig. 3*C*) and poorly folded (CD spectra in Supplemental Fig. 1*D*). Phe^{L32} was the only mutant at position 32 that demonstrated proper scFv folding. Although variant Phe^{L32} demonstrated some binding activity to the V3 loop peptide (Fig. 3*B*), it did not neutralize pseudotyped clade B HIV-1 (Fig. 3*C*). Hence, an aromatic residue at position 32 in the light chain is important for proper scFv folding but not necessarily for neutralization, where it seems that the phenoxy group is critical. Changes at position 27d do not affect scFv folding (Supplemental Fig. 1*B*) and appear to either have limited effect (with the exception of Ala^{L27d} and Gln^{L27d}) or even enhance binding to the V3 loop (Fig. 3*B*). The loss of V3 loop binding and neutralization ability of the Ala^{L27d} KD-247 scFv variant is consistent with the proposed role of Asn^{L27} in interacting with Arg^{315}. However, the only variant that was able to efficiently neutralize pseudotyped clade B HIV-1 was Asp^{L27d} (Fig. 3*C*). It is likely that the Glu^{L27d} and Gln^{L27d} variants are not as efficient in neutralization of pseudotyped virus because of their longer side chains

(as compared to Asp^{L27d} and Asn^{L27d}). Similarly, the even longer side chains of Arg^{L27d} and Lys^{L27d} are likely to negatively affect interactions with Arg^{315} because of steric constraints. The ability of the N27dD variant to neutralize clade B HIV-1 suggests that KD-247 may be substituted with Asp^{L27d} to retain activity against clade B HIV. This substitution would still be able to participate in the intricate network of hydrogen bond interactions proposed in our model for recognition of Arg^{315}. Although many of the scFv variants at position 92 of the light chain demonstrated proper folding (Supplemental Fig. 1*C*), Phe^{L92} demonstrated enhanced binding to the clade B V3 loop peptide while Ala^{L92} and Arg^{L92} had similar binding compared to the WT scFv (Fig. 3*B*), but only Phe^{L92} showed effective neutralization of clade B HIV-1 Env pseudotyped virus (Fig. 3*C*). These results establish that the aromatic ring at Tyr^{L92} is essential for clade B V3 loop recognition. Overall, these observations highlight the importance of Asn^{L27d}, Tyr^{L32}, and Tyr^{L92} in neutralizing clade B HIV-1 containing a GPGR V3 loop arch. Importantly, these results reveal that binding of scFv variants to clade B V3 loop peptides does not necessarily correlate with efficient HIV-1 clade B neutralization. It is possible that other factors may affect binding of the antibody in the context of the full Env glycoprotein that do not factor in to V3 peptide binding. The recent crystal structure of the native Env trimer by Julien *et al.* (71) revealed that the gp120 subunits are stabilized by β-hairpin interactions of the V3 loop and the V1/V2 strands B and C near the top of the trimer. The arch of the V3 loop is hidden by an *N*-acetyl glucosamine from the Asn^{197} glycan at the C-terminal region of V2 strand D from a neighboring protomer. This glycan blocks access to the V3 arch and may affect mAb binding.

Our findings are in agreement with previous work highlighting the dramatic flexibility of V3 loop and underscore the challenges in engineering antibodies that will be useful for treatment and vaccine design. Antibody engineering based on the interactions reported in our and other structures may lead to enhanced interactions with both Arg and Gln residues at position 315 of the V3 loop. For example, we expect that mutations of KD-247 residue Asn^{L27d} to longer polar residues (N27dQ, N27dK, and N27dR) should maintain the hydrogen bond interaction with clade B Arg^{315} and also be able to hydrogen bond with the shorter non–clade B Gln^{315}. Additionally, mutations of KD-247 residue Asp^{L28} to long polar residues (D28K, D28R, and D28E) should reach and interact with both clade B Arg^{315} and non–clade B Gln^{315}. Similarly, the Y32R mutant should maintain van der Waals interactions with clade B Arg^{315} and also make hydrogen bond interactions with non–clade B Gln^{315}. Combinations of the above mutations in the 27d, 28, 32, and 92 positions of the light chain of KD-247 may also help to maintain interactions with Arg^{315} and improve interactions with Gln^{315}. Additional approaches may include mutations of other KD-247 residues that do not interact directly with residue 315 of the V3 loop. Such interactions are observed in the structures of the 2557 and 3074 Fabs (22, 60) in complex with the V3 loop. Finally, extended CDR H3 loops may be designed to make nonspecific main chain interactions with the V3 loop, as is the case with 447-52D (61) and 537-10D (59), which form three-stranded and four-stranded antiparallel β-sheets with the V3 loop target.

Although the propensity of V3 loop to serve as an immunogen to elicit broadly neutralizing antibodies against HIV-1 of multiple clades has been challenging, the extensive studies performed by the Zolla-Pazner, Gorny, Wilson, and Kong groups suggest that this strategy may be achievable (22, 25, 55, 58–61, 69, 70, 72). FJ

The authors thank Dr. Jay Nix of ALS beamline 4.2.2 for assistance with data collection. The Advanced Light Source is supported by the director of the Office of Science, Office of Basic Energy Sciences, U.S. Department of Energy, under contract DE-AC02-05CH11231. A portion of the crystal structure of the unliganded KD-247 Fab was solved with guidance provided at the workshop entitled "CCP4 School: From Data Processing to Structure Refinement and Beyond" at Argonne National Laboratory (*http://www.ccp4.ac.uk/schools/APS-2008/index.php*) attended by K.A.K. The authors thank Drs. Krishna K. Sharma and Puttur Santhoshkumar for assistance with CD data collection. This work was supported, in whole or in part, by U.S. National Institutes of Health Grants AI076119, AI094715, AI099284, AI100890, AI112417, and GM103368 (S.G.S.). We also acknowledge support from the Ministry of Knowledge and Economy, Bilateral International Collaborative R&D Program, Republic of Korea. L.A.C. is supported by the MU-HHMI C^3 Program. B.M. is a recipient of the amfAR Mathilde Krim Fellowship and a Canadian Institutes of Health Research Fellowship.

REFERENCES

1. Le Douce, V., Janossy, A., Hallay, H., Ali, S., Riclet, R., Rohr, O., and Schwartz, C. (2012) Achieving a cure for HIV infection: do we have reasons to be optimistic? *J. Antimicrob. Chemother.* **67**, 1063–1074
2. Wei, X., Decker, J. M., Wang, S., Hui, H., Kappes, J. C., Wu, X., Salazar-Gonzalez, J. F., Salazar, M. G., Kilby, J. M., Saag, M. S., Komarova, N. L., Nowak, M. A., Hahn, B. H., Kwong, P. D., and Shaw, G. M.(2003) Antibody neutralization and escape by HIV-1. *Nature* **422**, 307–312
3. Parren, P. W., Burton, D. R., and Sattentau, Q. J. (1997) HIV-1 antibody—debris or virion? *Nat. Med.* **3**, 366–367
4. Yusim, K., Korber, B. T. M., Brander, C., Barouch, D., de Boer, R., Haynes, B. F., Koup, R., Moore, J. P., Walker, B. D., and Watkins, D. I. (2011) HIV Molecular Immunology, Los Alamos National Laboratory, Theoretical Biology and Biophysics, Los Alamos, New Mexico, http://www.hiv.lanl.gov/content/immunology
5. Burton, D. R., Barbas III, C. F., Persson, M. A., Koenig, S., Chanock, R. M., and Lerner, R. A. (1991) A large array of human monoclonal antibodies to type 1 human immunodeficiency virus from combinatorial libraries of asymptomatic seropositive individuals. *Proc. Natl. Acad. Sci. USA* **88**, 10134–10137
6. Trkola, A., Purtscher, M., Muster, T., Ballaun, C., Buchacher, A., Sullivan, N., Srinivasan, K., Sodroski, J., Moore, J. P., and Katinger, H. (1996) Human monoclonal antibody 2G12 defines a distinctive neutralization epitope on the gp120 glycoprotein of human immunodeficiency virus type 1. *J. Virol.* **70**, 1100–1108
7. Stiegler, G., Kunert, R., Purtscher, M., Wolbank, S., Voglauer, R., Steindl, F., and Katinger, H. (2001) A potent cross-clade neutralizing human monoclonal antibody against a novel epitope on gp41 of human immunodeficiency virus type 1. *AIDS Res. Hum. Retroviruses* **17**, 1757–1765
8. Barbato, G., Bianchi, E., Ingallinella, P., Hurni, W. H., Miller, M. D., Ciliberto, G., Cortese, R., Bazzo, R., Shiver, J. W., and Pessi, A. (2003) Structural analysis of the epitope of the anti-HIV antibody 2F5 sheds light into its mechanism of neutralization and HIV fusion. *J. Mol. Biol.* **330**, 1101–1115

9. Walker, L. M., Phogat, S. K., Chan-Hui, P. Y., Wagner, D., Phung, P., Goss, J. L., Wrin, T., Simek, M. D., Fling, S., Mitcham, J. L., Lehrman, J. K., Priddy, F. H., Olsen, O. A., Frey, S. M., Hammond, P. W.; Protocol G Principal Investigators, Kaminsky, S., Zamb, T., Moyle, M., Koff, W. C., Poignard, P., and Burton, D. R. (2009) Broad and potent neutralizing antibodies from an African donor reveal a new HIV-1 vaccine target. *Science* **326**, 285–289
10. Wu, X., Yang, Z. Y., Li, Y., Hogerkorp, C. M., Schief, W. R., Seaman, M. S., Zhou, T., Schmidt, S. D., Wu, L., Xu, L., Longo, N. S., McKee, K., O'Dell, S., Louder, M. K., Wycuff, D. L., Feng, Y., Nason, M., Doria-Rose, N., Connors, M., Kwong, P. D., Roederer, M., Wyatt, R. T., Nabel, G. J., and Mascola, J. R. (2010) Rational design of envelope identifies broadly neutralizing human monoclonal antibodies to HIV-1. *Science* **329**, 856–861
11. Walker, L. M., Huber, M., Doores, K. J., Falkowska, E., Pejchal, R., Julien, J. P., Wang, S. K., Ramos, A., Chan-Hui, P. Y., Moyle, M., Mitcham, J. L., Hammond, P. W., Olsen, O. A., Phung, P., Fling, S., Wong, C. H., Phogat, S., Wrin, T., Simek, M. D., Protocol G Principal Investigators, Koff, W. C., Wilson, I. A., Burton, D. R., and Poignard, P. (2011) Broad neutralization coverage of HIV by multiple highly potent antibodies. *Nature* **477**, 466–470
12. Scheid, J. F., Mouquet, H., Ueberheide, B., Diskin, R., Klein, F., Oliveira, T. Y., Pietzsch, J., Fenyo, D., Abadir, A., Velinzon, K., Hurley, A., Myung, S., Boulad, F., Poignard, P., Burton, D. R., Pereyra, F., Ho, D. D., Walker, B. D., Seaman, M. S., Bjorkman, P. J., Chait, B. T., and Nussenzweig, M. C. (2011) Sequence and structural convergence of broad and potent HIV antibodies that mimic CD4 binding. *Science* **333**, 1633–1637
13. Huang, J., Ofek, G., Laub, L., Louder, M. K., Doria-Rose, N. A., Longo, N. S., Imamichi, H., Bailer, R. T., Chakrabarti, B., Sharma, S. K., Alam, S. M., Wang, T., Yang, Y., Zhang, B., Migueles, S. A., Wyatt, R., Haynes, B. F., Kwong, P. D., Mascola, J. R., and Connors, M. (2012) Broad and potent neutralization of HIV-1 by a gp41-specific human antibody. *Nature* **491**, 406–412
14. Checkley, M. A., Luttge, B. G., and Freed, E. O. (2011) HIV-1 envelope glycoprotein biosynthesis, trafficking, and incorporation. *J. Mol. Biol.* **410**, 582–608
15. Berger, E. A., Murphy, P. M., and Farber, J. M. (1999) Chemokine receptors as HIV-1 coreceptors: roles in viral entry, tropism, and disease. *Annu. Rev. Immunol.* **17**, 657–700
16. Javaherian, K., Langlois, A. J., McDanal, C., Ross, K. L., Eckler, L. I., Jellis, C. L., Profy, A. T., Rusche, J. R., Bolognesi, D. P., Putney, S. D., et al. (1989) Principal neutralizing domain of the human immunodeficiency virus type 1 envelope protein. *Proc. Natl. Acad. Sci. USA* **86**, 6768–6772
17. Matsushita, S., Robert-Guroff, M., Rusche, J., Koito, A., Hattori, T., Hoshino, H., Javaherian, K., Takatsuki, K., and Putney, S. (1988) Characterization of a human immunodeficiency virus neutralizing monoclonal antibody and mapping of the neutralizing epitope. *J. Virol.* **62**, 2107–2114
18. Rusche, J. R., Javaherian, K., McDanal, C., Petro, J., Lynn, D. L., Grimaila, R., Langlois, A., Gallo, R. C., Arthur, L. O., Fischinger, P. J., et al. (1988) Antibodies that inhibit fusion of human immunodeficiency virus-infected cells bind a 24-amino acid sequence of the viral envelope, gp120. *Proc. Natl. Acad. Sci. USA* **85**, 3198–3202
19. Lynch, R. M., Shen, T., Gnanakaran, S., and Derdeyn, C. A. (2009) Appreciating HIV type 1 diversity: subtype differences in Env. *AIDS Res. Hum. Retroviruses* **25**, 237–248
20. Gorny, M. K., Williams, C., Volsky, B., Revesz, K., Cohen, S., Polonis, V. R., Honnen, W. J., Kayman, S. C., Krachmarov, C., Pinter, A., and Zolla-Pazner, S. (2002) Human monoclonal antibodies specific for conformation-sensitive epitopes of V3 neutralize human immunodeficiency virus type 1 primary isolates from various clades. *J. Virol.* **76**, 9035–9045
21. Pantophlet, R., Aguilar-Sino, R. O., Wrin, T., Cavacini, L. A., and Burton, D. R. (2007) Analysis of the neutralization breadth of the anti-V3 antibody F425-B4e8 and re-assessment of its epitope fine specificity by scanning mutagenesis. *Virology* **364**, 441–453
22. Hioe, C. E., Wrin, T., Seaman, M. S., Yu, X., Wood, B., Self, S., Williams, C., Gorny, M. K., and Zolla-Pazner, S. (2010) Anti-V3 monoclonal antibodies display broad neutralizing activities against multiple HIV-1 subtypes. *PLoS ONE* **5**, e10254
23. Conley, A. J., Gorny, M. K., Kessler II, J. A., Boots, L. J., Ossorio-Castro, M., Koenig, S., Lineberger, D. W., Emini, E. A., Williams, C., and Zolla-Pazner, S. (1994) Neutralization of primary human immunodeficiency virus type 1 isolates by the broadly reactive anti-V3 monoclonal antibody, 447-52D. *J. Virol.* **68**, 6994–7000
24. Gorny, M. K., Conley, A. J., Karwowska, S., Buchbinder, A., Xu, J. Y., Emini, E. A., Koenig, S., and Zolla-Pazner, S. (1992) Neutralization of diverse human immunodeficiency virus type 1 variants by an anti-V3 human monoclonal antibody. *J. Virol.* **66**, 7538–7542
25. Gorny, M. K., Williams, C., Volsky, B., Revesz, K., Wang, X. H., Burda, S., Kimura, T., Konings, F. A., Nádas, A., Anyangwe, C. A., Nyambi, P., Krachmarov, C., Pinter, A., and Zolla-Pazner, S. (2006) Cross-clade neutralizing activity of human anti-V3 monoclonal antibodies derived from the cells of individuals infected with non-B clades of human immunodeficiency virus type 1. *J. Virol.* **80**, 6865–6872
26. van Gils, M. J., and Sanders, R. W. (2013) Broadly neutralizing antibodies against HIV-1: templates for a vaccine. *Virology* **435**, 46–56
27. Eda, Y., Takizawa, M., Murakami, T., Maeda, H., Kimachi, K., Yonemura, H., Koyanagi, S., Shiosaki, K., Higuchi, H., Makizumi, K., Nakashima, T., Osatomi, K., Tokiyoshi, S., Matsushita, S., Yamamoto, N., and Honda, M. (2006) Sequential immunization with V3 peptides from primary human immunodeficiency virus type 1 produces cross-neutralizing antibodies against primary isolates with a matching narrow-neutralization sequence motif. *J. Virol.* **80**, 5552–5562
28. Matsushita, S., Takahama, S., Shibata, J., Kimura, T., Shiozaki, K., Eda, Y., Koito, A., Murakami, T., and Yoshimura, K. (2005) Ex vivo neutralization of HIV-1 quasi-species by a broadly reactive humanized monoclonal antibody KD-247. *Hum. Antibodies* **14**, 81–88
29. Eda, Y., Murakami, T., Ami, Y., Nakasone, T., Takizawa, M., Someya, K., Kaizu, M., Izumi, Y., Yoshino, N., Matsushita, S., Higuchi, H., Matsui, H., Shinohara, K., Takeuchi, H., Koyanagi, Y., Yamamoto, N., and Honda, M. (2006) Anti-V3 humanized antibody KD-247 effectively suppresses ex vivo generation of human immunodeficiency virus type 1 and affords sterile protection of monkeys against a heterologous simian/human immunodeficiency virus infection. *J. Virol.* **80**, 5563–5570
30. Murakami, T., Eda, Y., Nakasone, T., Ami, Y., Someya, K., Yoshino, N., Kaizu, M., Izumi, Y., Matsui, H., Shinohara, K., Yamamoto, N., and Honda, M. (2009) Postinfection passive transfer of KD-247 protects against simian/human immunodeficiency virus–induced $CD4^+$ T-cell loss in macaque lymphoid tissue. *AIDS* **23**, 1485–1494
31. Pflugrath, J. W. (1999) The finer things in X-ray diffraction data collection. *Acta Crystallogr. D Biol. Crystallogr.* **55**, 1718–1725
32. Matthews, B. W. (1985) Determination of protein molecular weight, hydration, and packing from crystal density. *Methods Enzymol.* **114**, 176–187
33. Vagin, A., and Teplyakov, A. (1997) MOLREP: an automated program for molecular replacement. *J. Appl. Cryst.* **30**, 1022–1025
34. Adams, P. D., Afonine, P. V., Bunkóczi, G., Chen, V. B., Davis, I. W., Echols, N., Headd, J. J., Hung, L. W., Kapral, G. J., Grosse-Kunstleve, R. W., McCoy, A. J., Moriarty, N. W., Oeffner, R., Read, R. J., Richardson, D. C., Richardson, J. S., Terwilliger, T. C., and Zwart, P. H. (2010) PHENIX: a comprehensive Python-based system for macromolecular structure solution. *Acta Crystallogr. D Biol. Crystallogr.* **66**, 213–221
35. Langer, G., Cohen, S. X., Lamzin, V. S., and Perrakis, A. (2008) Automated macromolecular model building for X-ray crystallography using ARP/wARP version 7. *Nat. Protoc.* **3**, 1171–1179
36. Murshudov, G. N., Vagin, A. A., and Dodson, E. J. (1997) Refinement of macromolecular structures by the maximum-likelihood method. *Acta Crystallogr. D Biol. Crystallogr.* **53**, 240–255
37. Emsley, P., Lohkamp, B., Scott, W. G., and Cowtan, K. (2010) Features and development of Coot. *Acta Crystallogr. D Biol. Crystallogr.* **66**, 486–501
38. Ong, Y. T., Kirby, K. A., Hachiya, A., Chiang, L. A., Marchand, B., Yoshimura, K., Murakami, T., Singh, K., Matsushita, S., and Sarafianos, S. G. (2012) Preparation of biologically active single-chain variable antibody fragments that target the HIV-1 gp120 V3 loop. *Cell. Mol. Biol. (Noisy-le-grand)* **58**, 71–79
39. Sreerama, N., and Woody, R. W. (1993) A self-consistent method for the analysis of protein secondary structure from circular dichroism. *Anal. Biochem.* **209**, 32–44

40. Sreerama, N., Venyaminov, S. Y., and Woody, R. W. (1999) Estimation of the number of alpha-helical and beta-strand segments in proteins using circular dichroism spectroscopy. *Protein Sci.* **8**, 370–380
41. Andrade, M. A., Chacón, P., Merelo, J. J., and Morán, F. (1993) Evaluation of secondary structure of proteins from UV circular dichroism spectra using an unsupervised learning neural network. *Protein Eng.* **6**, 383–390
42. Whitmore, L., and Wallace, B. A. (2004) DICHROWEB, an online server for protein secondary structure analyses from circular dichroism spectroscopic data. *Nucleic Acids Res.* **32**, W668-73
43. Whitmore, L., and Wallace, B. A. (2008) Protein secondary structure analyses from circular dichroism spectroscopy: methods and reference databases. *Biopolymers* **89**, 392–400
44. Janes, R. W. (2009) Reference datasets for protein ciruclar dichroism and synchrotron radiation circular dichroism spectroscopic analyses. In *Modern Techniques in Circular Dichroism and Synchrotron Radiation Circular Dichroism Spectroscopy,* Vol. 1, *Advances in Biomedical Spectroscopy* (Wallace, B. A., and Janes, R. W., eds.), pp. 183–201, IOS Press, Amsterdam, Netherlands
45. Shaw, G. M., Hahn, B. H., Arya, S. K., Groopman, J. E., Gallo, R. C., and Wong-Staal, F. (1984) Molecular characterization of human T-cell leukemia (lymphotropic) virus type III in the acquired immune deficiency syndrome. *Science* **226**, 1165–1171
46. Gallo, R. C., Salahuddin, S. Z., Popovic, M., Shearer, G. M., Kaplan, M., Haynes, B. F., Palker, T. J., Redfield, R., Oleske, J., Safai, B., et al. (1984) Frequent detection and isolation of cytopathic retroviruses (HTLV-III) from patients with AIDS and at risk for AIDS. *Science* **224**, 500–503
47. Montefiori, D. C. (2009) Measuring HIV neutralization in a luciferase reporter gene assay. *Methods Mol. Biol.* **485**, 395–405
48. Chen, V. B., Arendall III, W. B., Headd, J. J., Keedy, D. A., Immormino, R. M., Kapral, G. J., Murray, L. W., Richardson, J. S., and Richardson, D. C. (2010) MolProbity: all-atom structure validation for macromolecular crystallography. *Acta Crystallogr. D Biol. Crystallogr.* **66**, 12–21
49. Ramachandran, G. N., and Sasisekharan, V. (1968) Conformation of polypeptides and proteins. *Adv. Protein Chem.* **23**, 283–437
50. Stanfield, R. L., Zemla, A., Wilson, I. A., and Rupp, B. (2006) Antibody elbow angles are influenced by their light chain class. *J. Mol. Biol.* **357**, 1566–1574
51. Kabat, E. A., Wu, T. T., Perry, H. M., Gottesman, K. S., and Foeller, C. (1991) *Sequences of Proteins of Immunological Interest,* National Institutes of Health, Bethesda, MD
52. Abhinandan, K. R., and Martin, A. C. (2008) Analysis and improvements to Kabat and structurally correct numbering of antibody variable domains. *Mol. Immunol.* **45**, 3832–3839
53. Al-Lazikani, B., Lesk, A. M., and Chothia, C. (1997) Standard conformations for the canonical structures of immunoglobulins. *J. Mol. Biol.* **273**, 927–948
54. Shirai, H., Kidera, A., and Nakamura, H. (1996) Structural classification of CDR-H3 in antibodies. *FEBS Lett.* **399**, 1–8
55. Stanfield, R. L., Ghiara, J. B., Ollmann Saphire, E., Profy, A. T., and Wilson, I. A. (2003) Recurring conformation of the human immunodeficiency virus type 1 gp120 V3 loop. *Virology* **315**, 159–173
56. Ratner, L., Fisher, A., Jagodzinski, L. L., Mitsuya, H., Liou, R. S., Gallo, R. C., and Wong-Staal, F. (1987) Complete nucleotide sequences of functional clones of the AIDS virus. *AIDS Res. Hum. Retroviruses* **3**, 57–69
57. Javaherian, K., Langlois, A. J., LaRosa, G. J., Profy, A. T., Bolognesi, D. P., Herlihy, W. C., Putney, S. D., and Matthews, T. J. (1990) Broadly neutralizing antibodies elicited by the hypervariable neutralizing determinant of HIV-1. *Science* **250**, 1590–1593
58. Bell, C. H., Pantophlet, R., Schiefner, A., Cavacini, L. A., Stanfield, R. L., Burton, D. R., and Wilson, I. A. (2008) Structure of antibody F425-B4e8 in complex with a V3 peptide reveals a new binding mode for HIV-1 neutralization. *J. Mol. Biol.* **375**, 969–978
59. Burke, V., Williams, C., Sukumaran, M., Kim, S. S., Li, H., Wang, X. H., Gorny, M. K., Zolla-Pazner, S., and Kong, X. P. (2009) Structural basis of the cross-reactivity of genetically related human anti-HIV-1 mAbs: implications for design of V3-based immunogens. *Structure* **17**, 1538–1546
60. Jiang, X., Burke, V., Totrov, M., Williams, C., Cardozo, T., Gorny, M. K., Zolla-Pazner, S., and Kong, X. P. (2010) Conserved structural elements in the V3 crown of HIV-1 gp120. *Nat. Struct. Mol. Biol.* **17**, 955–961
61. Stanfield, R. L., Gorny, M. K., Williams, C., Zolla-Pazner, S., and Wilson, I. A. (2004) Structural rationale for the broad neutralization of HIV-1 by human monoclonal antibody 447-52D. *Structure* **12**, 193–204
62. Yoshimura, K., Shibata, J., Kimura, T., Honda, A., Maeda, Y., Koito, A., Murakami, T., Mitsuya, H., and Matsushita, S. (2006) Resistance profile of a neutralizing anti-HIV monoclonal antibody, KD-247, that shows favourable synergism with anti-CCR5 inhibitors. *AIDS* **20**, 2065–2073
63. Hatada, M., Yoshimura, K., Harada, S., Kawanami, Y., Shibata, J., and Matsushita, S. (2010) Human immunodeficiency virus type 1 evasion of a neutralizing anti-V3 antibody involves acquisition of a potential glycosylation site in V2. *J. Gen. Virol.* **91**, 1335–1345
64. Kessler, N., Zvi, A., Ji, M., Sharon, M., Rosen, O., Levy, R., Gorny, M., Zolla-Pazner, S., and Anglister, J. (2003) Expression, purification, and isotope labeling of the Fv of the human HIV-1 neutralizing antibody 447-52D for NMR studies. *Protein Expr. Purif.* **29**, 291–303
65. Brändén, C., and Tooze, J. (1999) *Introduction to Protein Structure,* Garland Science, New York
66. Greenfield, N., and Fasman, G. D. (1969) Computed circular dichroism spectra for the evaluation of protein conformation. *Biochemistry* **8**, 4108–4116
67. Eglen, R. M., Reisine, T., Roby, P., Rouleau, N., Illy, C., Bossé, R., and Bielefeld, M. (2008) The use of AlphaScreen technology in HTS: current status. *Curr. Chem. Genomics* **1**, 2–10
68. Sundberg, E. J. (2009) Structural basis of antibody-antigen interactions. *Methods Mol. Biol.* **524**, 23–36
69. Stanfield, R. L., Gorny, M. K., Zolla-Pazner, S., and Wilson, I. A. (2006) Crystal structures of human immunodeficiency virus type 1 (HIV-1) neutralizing antibody 2219 in complex with three different V3 peptides reveal a new binding mode for HIV-1 cross-reactivity. *J. Virol.* **80**, 6093–6105
70. Gorny, M. K., Xu, J. Y., Karwowska, S., Buchbinder, A., and Zolla-Pazner, S. (1993) Repertoire of neutralizing human monoclonal antibodies specific for the V3 domain of HIV-1 gp120. *J. Immunol.* **150**, 635–643
71. Julien, J. P., Cupo, A., Sok, D., Stanfield, R. L., Lyumkis, D., Deller, M. C., Klasse, P. J., Burton, D. R., Sanders, R. W., Moore, J. P., Ward, A. B., and Wilson, I. A. (2013) Crystal structure of a soluble cleaved HIV-1 envelope trimer. *Science* **342**, 1477–1483
72. Gorny, M. K., Revesz, K., Williams, C., Volsky, B., Louder, M. K., Anyangwe, C. A., Krachmarov, C., Kayman, S. C., Pinter, A., Nadas, A., Nyambi, P. N., Mascola, J. R., and Zolla-Pazner, S. (2004) The v3 loop is accessible on the surface of most human immunodeficiency virus type 1 primary isolates and serves as a neutralization epitope. *J. Virol.* **78**, 2394–2404

Received for publication June 6, 2014.
Accepted for publication August 26, 2014.

Journal of General Virology (2014), 95, 1816–1826 DOI 10.1099/vir.0.062885-0

Impact of maraviroc-resistant and low-CCR5-adapted mutations induced by *in vitro* passage on sensitivity to anti-envelope neutralizing antibodies

Kazuhisa Yoshimura,[1,2]† Shigeyoshi Harada,[1,2]† Samatchaya Boonchawalit,[1,2] Yoko Kawanami[2] and Shuzo Matsushita[2]

Correspondence
Kazuhisa Yoshimura
ykazu@nih.go.jp
Shuzo Matsushita
shuzo@kumamoto-u.ac.jp

[1]AIDS Research Centre, National Institute of Infectious Diseases, 1-23-1 Toyama, Shinjuku-ku, Tokyo 162-8640, Japan

[2]Center for AIDS Research, Kumamoto University, 2-2-1 Honjo, Chuo-ku, Kumamoto 860-0811, Japan

The aim of this study was to generate maraviroc (MVC)-resistant viruses *in vitro* using a human immunodeficiency virus type 1 subtype B clinical isolate (HIV-1_{KP-5}) to understand the mechanism(s) of resistance to MVC. To select HIV-1 variants resistant to MVC *in vitro*, we exposed high-chemokine (C-C motif) receptor 5 (CCR5)-expressing PM1/CCR5 cells to HIV-1_{KP-5} followed by serial passage in the presence of MVC. We also passaged HIV-1_{KP-5} in PM1 cells, which were low CCR5 expressing to determine low-CCR5-adapted substitutions and compared the Env sequences of the MVC-selected variants. Following 48 passages with MVC (10 μM), HIV-1_{KP-5} acquired a resistant phenotype [maximal per cent inhibition (MPI) 24 %], whilst the low-CCR5-adapted variant had low sensitivity to MVC (IC_{50} ~200 nM), but not reduction of the MPI. The common substitutions observed in both the MVC-selected and low-CCR5-adapted variants were selected from the quasi-species, in V1, V3 and V5. After 14 passages, the MVC-selected variants harboured substitutions around the CCR5 N-terminal-binding site and V3 (V200I, T297I, K305R and M434I). The low-CCR5-adapted infectious clone became sensitive to anti-CD4bs and CD4i mAbs, but not to anti-V3 mAb and autologous plasma IgGs. Conversely, the MVC-selected clone became highly sensitive to the anti-envelope (Env) mAbs tested and the autologous plasma IgGs. These findings suggest that the four MVC-resistant mutations required for entry using MVC-bound CCR5 result in a conformational change of Env that is associated with a phenotype sensitive to anti-Env neutralizing antibodies.

Received 15 December 2013
Accepted 29 April 2014

INTRODUCTION

Human immunodeficiency virus type 1 (HIV-1) entry into target cells is triggered by the interaction of the viral envelope glycoproteins (Env) with its receptor CD4 and one or two major coreceptors, chemokine (C-C motif) receptor 5 (CCR5) or chemokine (C-X-C motif) receptor 4 (CXCR4), and culminates in fusion of the viral and cell membranes. Env is organized into trimers on virions, and consists of the gp120 surface and gp41 transmembrane subunits (Wyatt & Sodroski, 1998). The small-molecule CCR5 antagonist maraviroc (MVC) was the first CCR5 inhibitor licensed for clinical use (Gulick *et al.*, 2008). CCR5 inhibitors work by allosterically altering the conformation of CCR5 at the cell surface, thereby disrupting its interaction with HIV gp120 (Berger *et al.*, 1999; Dorr *et al.*, 2005). Although MVC and another CCR5 inhibitor, vicriviroc (VCV), can efficiently suppress HIV-1 replication, resistant variants can arise both *in vitro* and *in vivo*, and these resistant viruses are adapted to use drug-bound CCR5 for entry (Berro *et al.*, 2009; Kuhmann *et al.*, 2004; Marozsan *et al.*, 2005; Ogert *et al.*, 2009, 2010; Ratcliff *et al.*, 2013; Roche *et al.*, 2011b; Tilton *et al.*, 2010; Tsibris *et al.*, 2008; Westby *et al.*, 2007; Yuan *et al.*, 2011; Yusa *et al.*, 2005). Current models of gp120 binding to a coreceptor suggest that the crown of the gp120 V3 loop interacts principally with the second extracellular loop region of the coreceptor, whilst the gp120 bridging sheet, which is formed after CD4 binding, and the stem of the V3 loop interact with the N terminus of the coreceptor (Brelot *et al.*, 1999; Cormier & Dragic, 2002; Farzan *et al.*, 1999; Huang *et al.*, 2005). The development of resistance is an important issue for HIV treatment regimens incorporating MVC, as is the case for any antimicrobial agent.

†These authors contributed equally to this work.

The GenBank/EMBL/DDBJ accession numbers for the envelope sequences of KP-5 are AB742145–AB742157.

Three supplementary figures are available with the online version of this paper.

HIV-1 can develop clinical resistance to CCR5 antagonists by two routes. The first pathway is through emergence of pre-existing CXCR4-using viruses (Fätkenheuer *et al.*, 2008; Landovitz *et al.*, 2008; Westby *et al.*, 2006). CCR5 inhibitor evasion can also occur by the accumulation of multiple mutations in gp120 and/or gp41 without a switch in coreceptor usage (Dragic *et al.*, 2000; Maeda *et al.*, 2006, 2008a; Roche *et al.*, 2011b; Tsamis *et al.*, 2003). The resistant pathway is characterized not by shifts in IC_{50} (a competitive inhibitor), but rather by reductions in the maximal per cent inhibition (MPI). Reductions in MPI are due to the resistant virus developing the ability to bind to the antagonist-modified form of CCR5 (Westby *et al.*, 2007). However, one study reported that chimeric clones bearing the N425K mutation in C4 replicated at high MVC concentrations and displayed significant shifts in IC_{50}s, characteristic of resistance to all other antiretroviral drugs, but not MVC (Ratcliff *et al.*, 2013).

Escape mutants to the CCR5 inhibitor, AD101 (SCH-350581), have been found to be more sensitive than the parental isolate to a subset of neutralizing mAbs against V3 and a CD4-induced (CD4i) epitope (Pugach *et al.*, 2007; Berro *et al.*, 2009). To date, however, it is not clear which mutation(s) induced by MVC affect the accessibility of neutralizing mAbs to the epitopes in Env.

Therefore, to determine the resistance mechanisms to MVC, we passaged a primary CCR5-tropic (R5) subtype B isolate in the high-CCR5-expressing T-cell line PM1/CCR5 in the presence of MVC (Fig. S1, available in the online Supplementary Material) and compared the Env sequences of variants with those cultured in the low-CCR5-expressing parental PM1 cell line (Fig. S1). We also investigated the phenotypic change in the MVC-resistant clone against anti-Env antibodies, especially for anti-V3 neutralizing mAbs and autologous plasma IgGs, and compared the results with the low-CCR5-adapted clone to determine the key mutations for accessibility of neutralizing mAbs to the epitopes in Env.

RESULTS

Anti-HIV-1 activities of MVC toward laboratory strains and primary HIV-1 isolates

Initially, we determined the MPI and the IC_{50} values of MVC against different laboratory-adapted and primary HIV-1 isolates, including both CXCR4-tropic (X4) and R5 viruses. MVC inhibited the laboratory-adapted HIV-1 R5 strains HIV-1_{BaL} and HIV-$1_{JR\text{-}FL}$ with MPIs of 98 and 97 %, respectively, but did not inhibit the X4 virus HIV-1_{IIIB} or dual-tropic virus HIV-$1_{89.6}$ (MPI <20 %, Table 1). We also tested MVC against 14 R5 primary isolates, including subtypes B, C and G, and the circulating recombinant form CRF08_BC. MVC effectively inhibited all of these primary isolates at concentrations of 1.2–26 nM (MPI 92–100 %), but did not inhibit three primary X4 isolates (two CRF01_AE and one subtype B) with MPI <20 % (Table 1).

Table 1. Inhibitory activities of MVC toward infection by laboratory-adapted and primary strains of HIV-1

Virus	Subtype	IC_{50}* (nM)	MPI (%)
Laboratory adapted			
R5			
HIV-1_{BaL}	B	26	98
HIV-$1_{JR\text{-}FL}$	B	6.9	97
Dual			
HIV-$1_{89.6}$	B	>1000	<20
X4			
HIV-1_{IIIB}	B	>1000	<20
Primary			
R5			
HIV-$1_{KP\text{-}5}$	B	26	92
HIV-$1_{KP\text{-}2}$	CRF08_BC	24	95
HIV-$1_{KP\text{-}6}$	G	20	95
HIV-$1_{KP\text{-}7}$	B	18	95
HIV-$1_{KP\text{-}8}$	B	14	97
HIV-$1_{KP\text{-}9}$	B	13	96
HIV-$1_{KP\text{-}10}$	B	9.2	98
HIV-$1_{KP\text{-}11}$	C	8.6	96
HIV-$1_{KP\text{-}12}$	B	5.1	98
HIV-$1_{KP\text{-}13}$	B	4.0	96
HIV-$1_{KP\text{-}14}$	B	3.0	95
HIV-$1_{KP\text{-}15}$	B	3.0	94
HIV-$1_{KP\text{-}16}$	B	2.2	100
HIV-$1_{KP\text{-}17}$	B	1.2	98
X4/mix			
HIV-$1_{KP\text{-}18}$	CRF01_AE	>1000	<20
HIV-$1_{KP\text{-}19}$	CRF01_AE	>1000	<20
HIV-$1_{KP\text{-}20}$	B	>1000	<20

*PM1/CCR5 cells (2×10^3) were exposed to 100 $TCID_{50}$ of each virus and then cultured in the presence of various concentrations of MVC. The IC_{50} values were determined by the WST-8 assay using a Cell Counting kit-8 on day 7 of culture. All assays were conducted in duplicate or triplicate.

Selection of MVC-resistant variants

To select MVC-resistant HIV-1 variants *in vitro*, we exposed PM1/CCR5 cells to HIV-$1_{KP\text{-}5}$, which had the highest IC_{50} value (26 nM) and lowest MPI (92 %) among the primary isolates tested, and serially passaged the viruses in the presence of increasing concentrations of MVC. As a control, HIV-$1_{KP\text{-}5}$ was passaged under the same conditions without MVC in PM1/CCR5 cells (designated the passage control). Moreover, to compare the differences between the MVC-resistant variant and low-CCR5-expressing-cell-adapted variant, we passaged HIV-$1_{KP\text{-}5}$ in low-CCR5-expressing parental PM1 cells (designated low-CCR5-adapted). The selected virus was initially propagated in the presence of 1 nM MVC and during the course of the selection procedure the concentration of MVC was increased to 10 μM over 48 passages (Fig. 1a).

Resistance to small-molecule CCR5 inhibitors is known to vary according to the cell type used (Anastassopoulou

et al., 2009; Ogert *et al.*, 2008; Pugach *et al.*, 2007; Westby *et al.*, 2007). To characterize the resistance profiles of the passaged variants, we tested the sensitivities of the three variants and HIV-1_{BaL} to MVC in phytohaemagglutinin (PHA)-activated PBMCs (Fig. 1b). The MPI of the MVC-resistant variant was lower than the MPIs of the passage control, low-CCR5-adapted variant and HIV-1_{BaL} (MPI 80.3 versus 92.3, 94.5 and 95.7 %, respectively).

The MVC-selected variant became highly resistant to MVC (Fig. 2), with an MPI of 24 % at 48 passages. However, the low-CCR5-adapted variant, which was passaged in PM1 cells, became low sensitive to MVC compared with the passage control (IC_{50} 279 versus 26.3 nM), but we did not find a reduction in the MPI.

We also determined the sequential MPIs and IC_{50} values of each passaged variant to MVC (Fig. 2). From passages

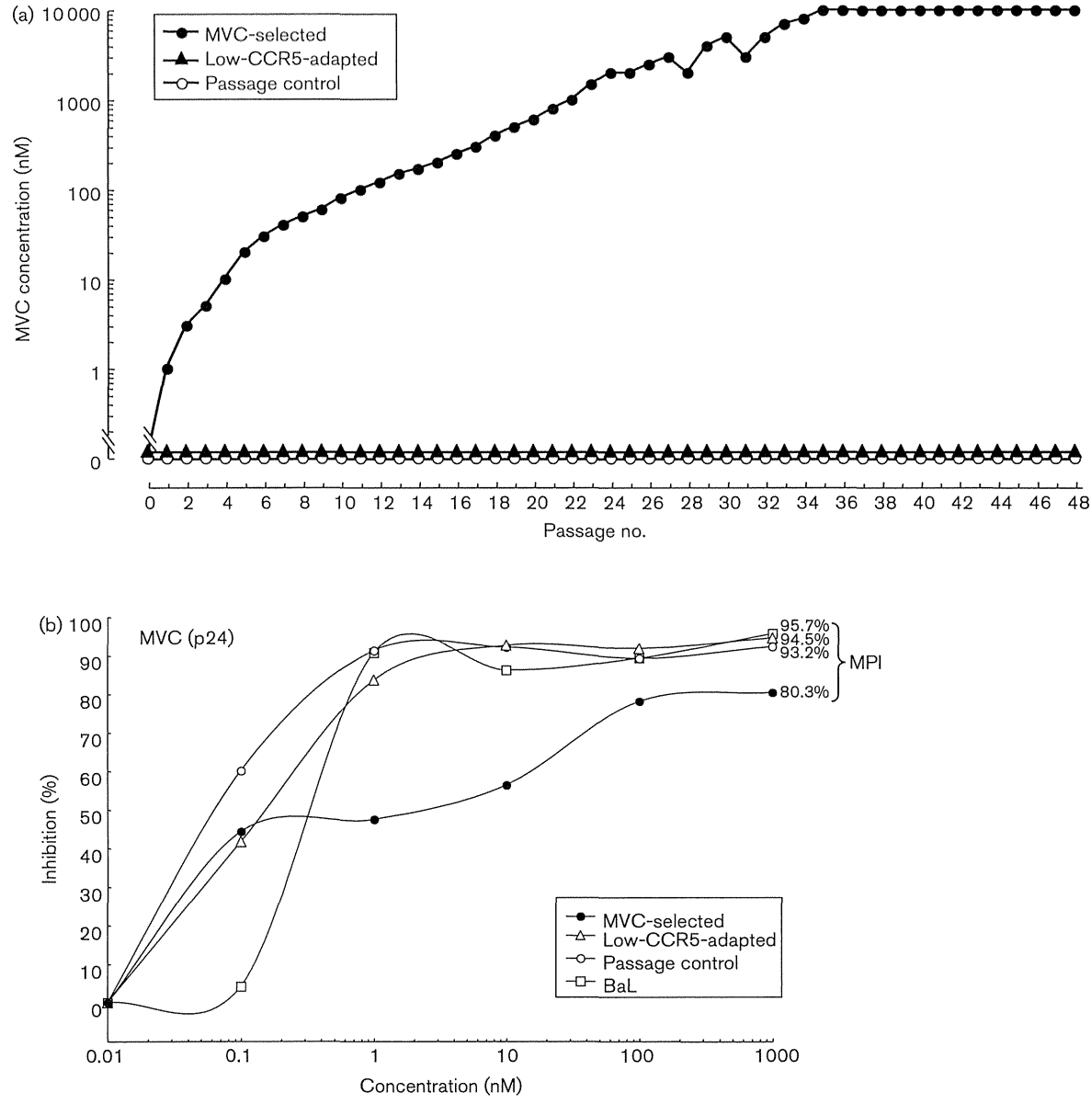

Fig. 1. Selection of MVC-resistant and low-CCR5-adapted virus variants. (a) The selection was carried out in PM1/CCR5 and PM1 cells as described in Methods. (b) Sensitivities of the MVC-selected (48 passages), low-CCR5-adapted (48 passages), passage control (48 passages) variants and HIV-1_{BaL} (BaL) to MVC as determined by p24 antigen measurement. PHA-activated PBMCs (1×10^6 cells ml^{-1}) were exposed to 100 $TCID_{50}$ of each variant and cultured in the presence or absence of various concentrations of the drug in 96-well microculture plates. The amounts of p24 antigen produced by the cells were determined on day 7. All assays were performed in triplicate.

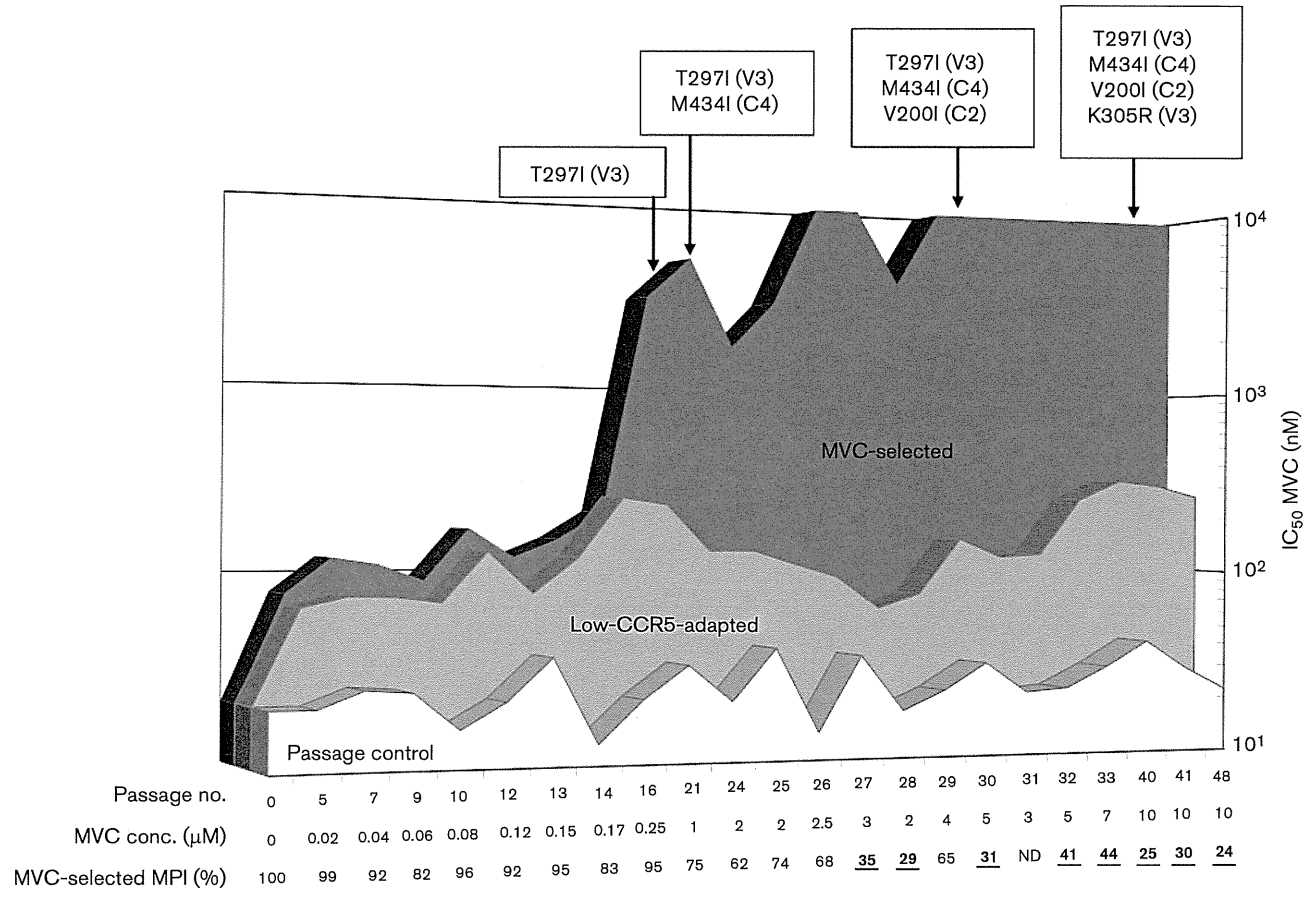

Fig. 2. Susceptibility of passaged variants to MVC. The sensitivity and MPI of each passaged variant to MVC was determined by a multi-round assay using the WST-8 assay as described in Methods. The *x*-axis shows the passage number, concentration of MVC (μM) and MPI values. The mutations observed in the highly MVC-resistant variants are shown above the graph.

1 to 14, the MVC-selected and low-CCR5-adapted variants had almost equal IC_{50} values and the MPIs were high. After 16 passages, the IC_{50} values of the MVC-selected variants continued to increase to >10 μM, whilst the MPIs decreased to 24% at 48 passages, especially after 27 passages. The low-CCR5-adapted variants maintained an IC_{50} value of ~200 nM and high MPIs (90–100%) until the end of the experiment (passage 48). Conversely, the passage control variants did not show remarkable changes in their IC_{50} values and MPIs throughout the passages (IC_{50} values of ~20 nM, MPI 95–100%). The low-CCR5-adapted variant was also resistant to two other CCR5 inhibitors, APL and TAK-779 (data not shown).

These findings suggested that the phenotype of the MVC-selected variants under low concentrations of the drug corresponded with that of the low-CCR5-adapted variants until 14 passages; then, under high concentrations, the MVC-selected variants acquired additional mutations for high resistance to the CCR5 inhibitor.

Comparison of the Env region sequences of the MVC-selected and low-CCR5-adapted mutants

To determine the genetic basis of the resistance in the HIV-1_{KP-5} variants and compare the substitutions between the MVC-selected and low-CCR5-adapted variants, the Env genes were sequenced (Figs 3, 4 and S2). At 17 passages, all substitutions in both the MVC-selected and low-CCR5-adapted variants were selected from the baseline viruses. Five of these substitutions in gp120, i.e. K8R, C11W (signal peptide), D141N (V1), E321D (V3) and I463T (V5), were observed in both passaged variants. Conversely, at positions 137 (K or E), 148 (Q or K) and 187 (G or D), the amino acids differed between the MVC-selected and low-CCR5-adapted variants. After 16 passages, the MVC-selected variants acquired four additional mutations, i.e. T297I (V3), M434I (C4), V200I (C2) and K305R (V3), at passages 17, 21, 34 and 41, respectively, which were not observed in the low-CCR5-adapted variants (Figs 2–4 and S2). After acquisition of M434I in C4 (21 passages), the MPI of the MVC-selected variants decreased gradually

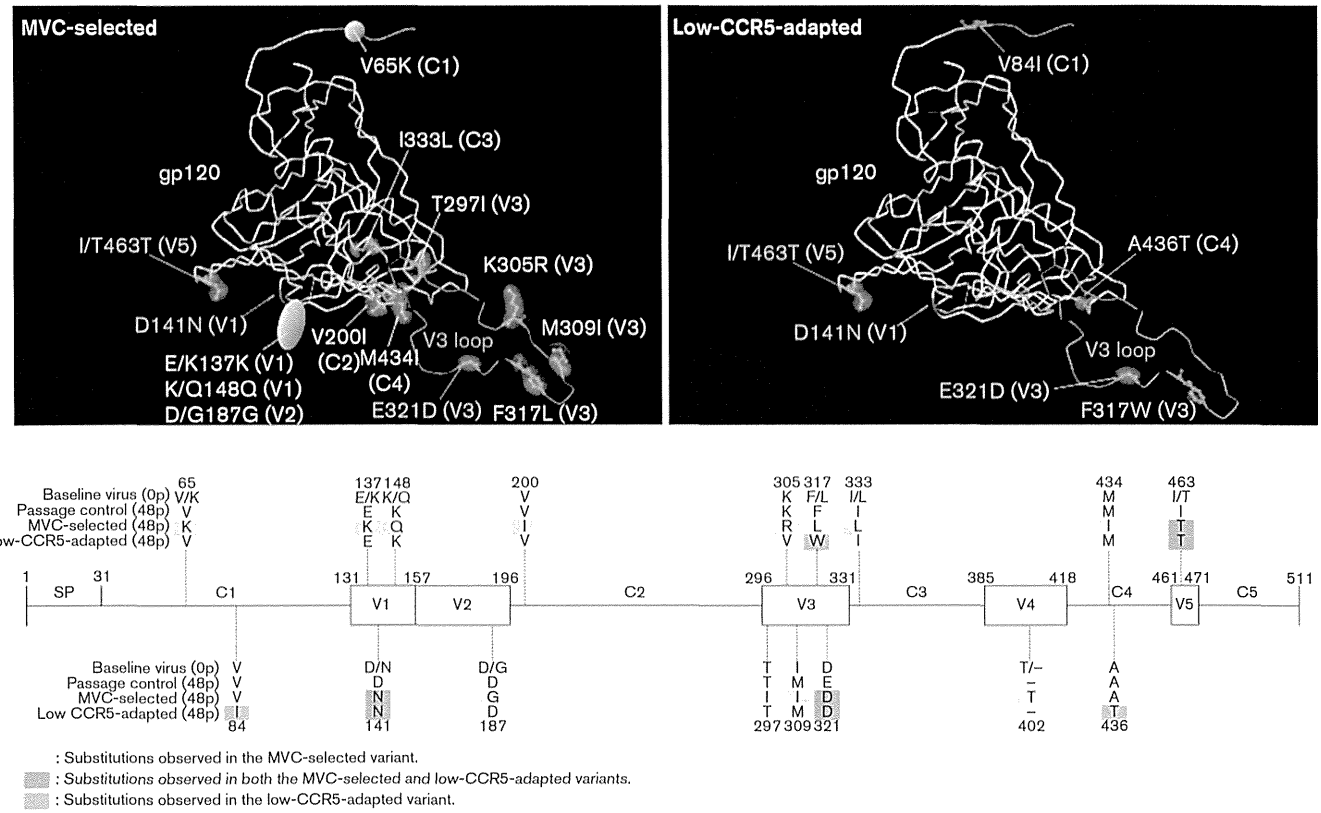

Fig. 3. Comparison of the locations of the mutations in the MVC-selected and low-CCR5-adapted gp120. The side chains of the mutated residues that appeared during the MVC selection (left) and low CCR5 adaptation (right) are shown in yellow (only MVC selection), pink (only low CCR5 adaptation) and green (both). A summary schema is also provided.

(from 74 to 24 %) (Fig. 2). The most important amino acid substitution for the reduction in the MPI might be K305R, because the MPI of the variant cultured without MVC after 48 passages increased by reverting from R to K at position 305 (data not shown). Three additional mutations, i.e. F317W (V3), V84I (C1) and A436T (C4), were observed in the low-CCR5-adapted variants at 17, 21 and 48 passages, respectively. These mutations might be compensatory for viral fitness following culture in the low-CCR5-expressing cells, because the MPIs of the variants with these three mutations did not differ from those of the variants prior to the acquisition of these mutations (>90 %).

These findings suggest that under low concentrations of MVC, the variants were selected from the baseline viruses similarly to the low-CCR5-adapted variants (IC_{50} shift and high MPI), whilst under high concentrations of the drug, the selected variants required additional mutations to use drug-bound coreceptors for entry into the target cells.

To compare the two mutation profiles obtained from the MVC-selected and low-CCR5-adapted variants at 48 passages, the crystal structure of gp120 was used (Figs 3 and 4). Comparison of the sequences of the two passaged variants based on the Protein Data Bank (PDB ID: 2B4C) crystal structure of gp120 showed that the MVC-selected variant harboured many substitutions within and around the V3 region, i.e. the CCR5 N-terminal-binding site, compared with the low-CCR5-adapted variant in the three-dimensional (3D) position. In a magnification of the CCR5 N-terminal-binding site (Fig. 4), three of four mutations, i.e. T297I, M434I and V200I, were concentrated around the V3 base and finally K305R appeared in the V3 stem region after 41 passages.

To determine the positions of MVC-selected mutations in the gp120 trimer form, we illustrated the sites of mutations on the structure of the BG505 SOSIP trimer obtained from the PDB (ID: 3J5M) (Fig. S3) (Lyumkis *et al.*, 2013). Almost all of the MVC-selected mutations occurred at the upper and outer side of the trimer. Several MVC-selected mutations, i.e. V65K, V200I, K305R, M309I, F317L and M434I, lay relatively close to the neighbouring gp120. These findings demonstrated that these mutations may affect trimer formation and expose neutralizing antibody epitopes.

Susceptibilities of the infectious clones with mutant Env to anti-Env mAbs

In a previous study, a CCR5 inhibitor (AD101)-resistant infectious clone was sensitive to neutralization via V3 and

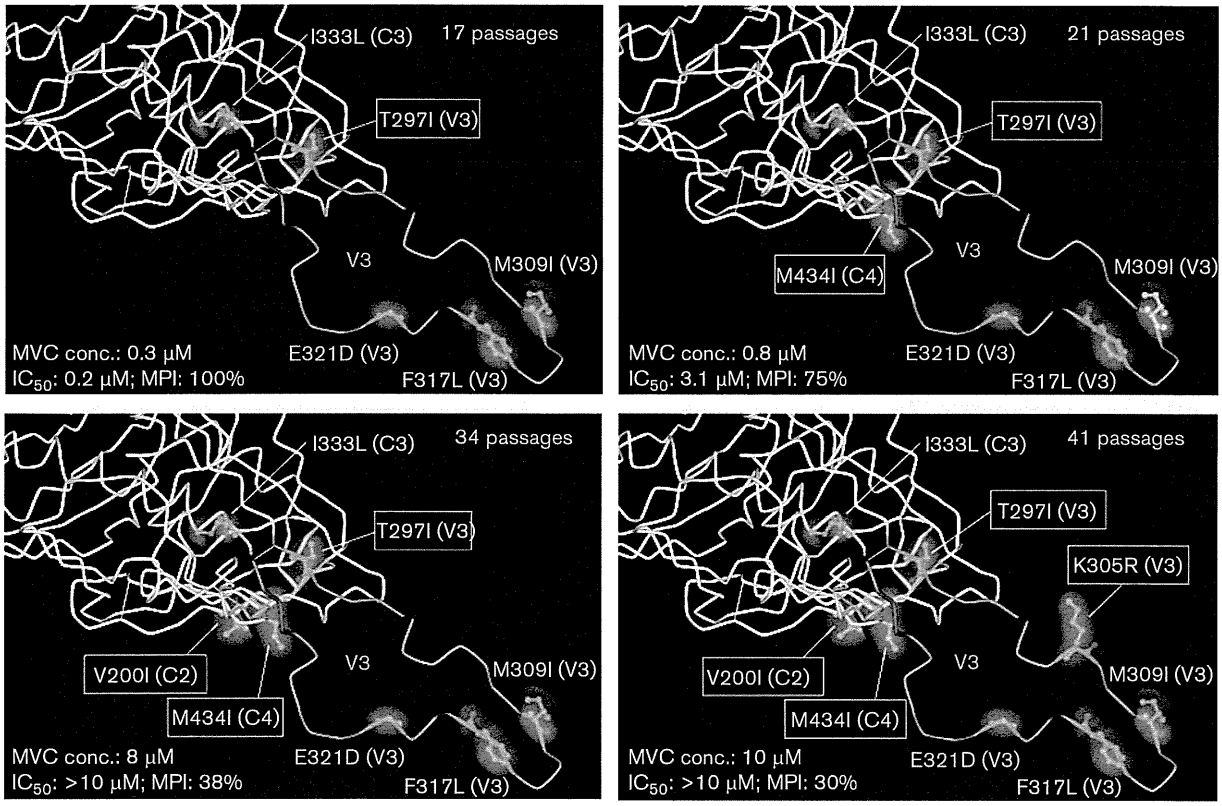

Fig. 4. Enlargement of the area of the CCR5 N-terminal-binding site and V3 loop in gp120. The side chains of the mutated residues that appeared during *in vitro* selection with MVC at 17 (upper left), 21 (upper right), 34 (lower left) and 41 passages (lower right) are shown. The crystal structure of gp120 was retrieved from the Protein Data Bank (PDB ID: 2B4C).

CD4i epitopes (Berro *et al.*, 2009). To examine whether our three passaged variants became sensitive to anti-Env mAbs, we constructed three infectious clones with each 48-passaged Env (Fig. 5). The clone with the Env of the MVC-selected variant showed a low MPI (56 %) under a high concentration of MVC, which was also seen with the passage control and low-CCR5-adapted clones (Fig. 5a). Using these infectious clones, we tested the susceptibilities to the anti-Env mAbs b12 [anti-CD4 binding site (anti-CD4bs)], 4E9C (anti-CD4i) and KD-247 (anti-V3). As shown in Fig. 5(b), the MVC-selected and low-CCR5-adapted clones showed higher sensitivity to b12 than the passage control clone, with IC_{50} values of 0.22, 0.31 and 0.86 μg ml^{-1}, respectively. The MVC-selected and low-CCR5-adapted clones became highly sensitive to 4E9C compared with the passage control clone (IC_{50} values of 0.08, 0.41 and >5 μg ml^{-1}, respectively) (Fig. 5c). Moreover, the clone with the MVC-selected Env was highly sensitive to anti-V3 mAb KD-247, while the low-CCR5-adapted and passage control clones were not (IC_{50} values of 0.04, >100 and >100 μg ml^{-1}, respectively) (Fig. 5d).

These findings indicated that the MVC-selected clone with its greater number of mutations might contribute to exposure of neutralizing epitopes for these three mAbs, whilst the low-CCR5-adapted mutations could change the conformation of Env to become sensitive to anti-CD4i and CD4bs mAbs, but not anti-V3 mAb.

Susceptibilities of the infectious clones with mutant Env to autologous plasma IgGs

We also examined whether the infectious clones with the passaged Env mutations were neutralized by autologous plasma IgGs. As shown in Fig. 6(a), none of the autologous plasma IgGs could neutralize the passage control clone at concentrations up to 100 μg ml^{-1}. In the low-CCR5-adapted clone, some of the plasma IgGs slightly inhibited the replication of the virus under high concentrations, but did not reach the 50 % inhibition level (Fig. 6b). Conversely, all seven plasma IgGs were able to completely neutralize the clone with the MVC-selected Env (IC_{50} 2.6–37 μg ml^{-1}, MPI 79–97 %) (Fig. 6c).

These findings show that the MVC-selected clone with the greater number of mutations also might contribute to exposure of neutralizing epitopes for autologous plasma IgGs.

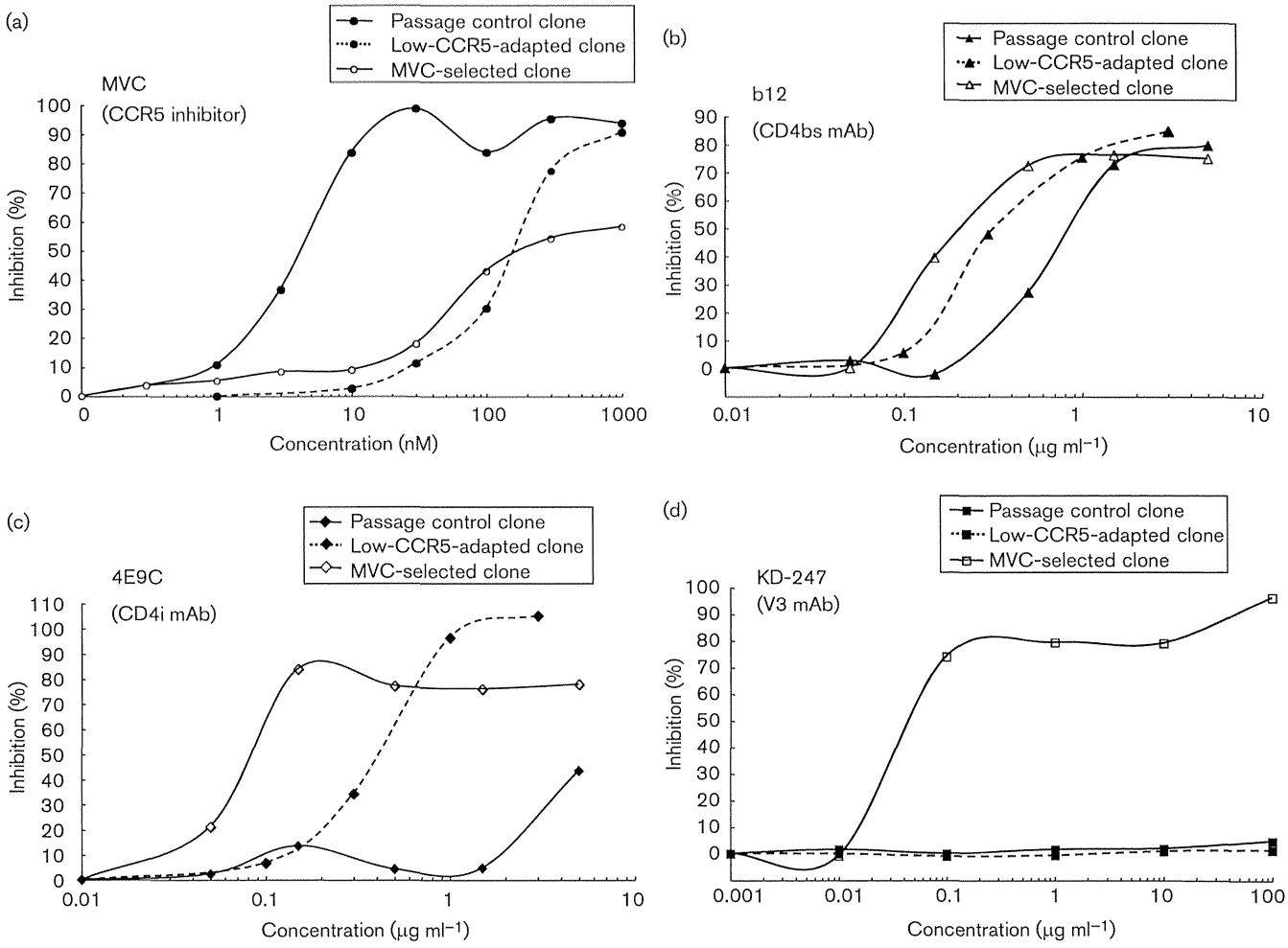

Fig. 5. Sensitivities of infectious clones with the passage control, low-CCR5-adapted and MVC-selected Env mutations to MVC and anti-Env mAbs. The sensitivities of the infectious clones with the passage control (filled symbols), low-CCR5-adapted (filled symbols and dotted lines) and MVC-selected (open symbols) Env mutations to (a) MVC, (b) b12, (c) 4E9C and (d) KD-247 are shown. The sensitivities of each infectious clone to MVC and mAbs were determined by the WST-8 assay as described in Methods. All assays were conducted in duplicate.

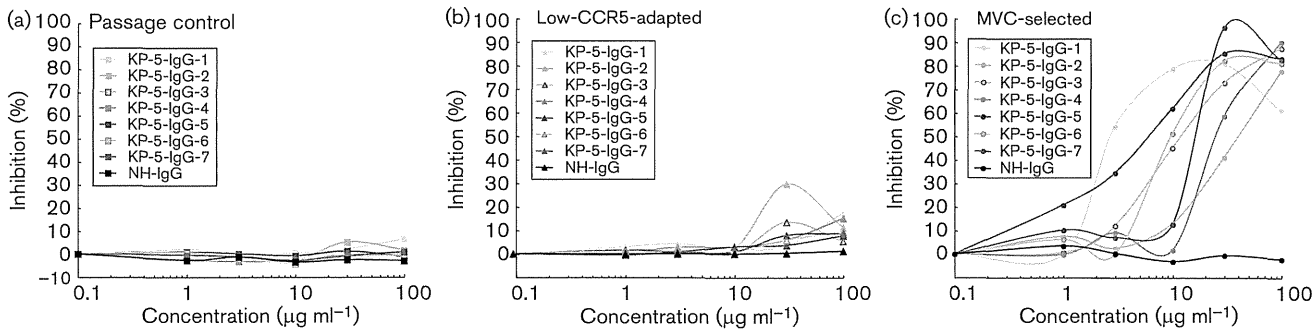

Fig. 6. Sensitivities of infectious clones with the passage control, low-CCR5-adapted and MVC-selected Env mutations to autologous plasma IgGs. The sensitivities of the infectious clones with the (a) passage control, (b) low-CCR5-adapted and (c) MVC-selected Env mutations to seven autologous plasma IgGs (KP-5-IgG-1 to KP-5-IgG-7; coloured symbols) and normal human plasma IgG (NH-IgG; black symbols) are shown. The sensitivity of each infectious clone to the plasma IgGs was determined by the WST-8 assay as described in Methods. All assays were conducted in duplicate.

DISCUSSION

The CCR5 inhibitors, MCV and VCV, are allosteric inhibitors of virus entry, hence resistance to these drugs is evidenced by a reduction in the plateau of virus inhibition curves rather than by increases in IC_{50} (Dragic *et al.*, 2000; Maeda *et al.*, 2006, 2008a; Roche *et al.*, 2011b; Tsamis *et al.*, 2003). One study reported that resistant mechanisms contribute to the altered recognition of drug-bound CCR5 by an MVC-resistant HIV-1 strain. This study demonstrated very efficient usage of drug-bound CCR5, characterized by increased dependence on the CCR5 N terminus (Tilton *et al.*, 2010). Another report demonstrated a similar yet distinct mechanism of escape from MVC by MVC-resistant Env, with comparatively less efficient usage of drug-bound CCR5 (Roche *et al.*, 2011b). In the absence of the drug, MVC-resistant Env maintains a highly efficient interaction with CCR5, similar to that of MVC-sensitive Env, and displays a relatively modest increase in dependence on the CCR5 N terminus (Roche *et al.*, 2011b). However, in the presence of the drug, MVC-resistant Env interacts much less efficiently with CCR5 and becomes critically dependent on the CCR5 N terminus. In the current study, we induced MVC-resistant HIV-1, which harboured many substitutions within and around the V3 region, i.e. the CCR5 N-terminal-binding site *in vitro*. In order to determine whether the resistant variant displayed an increased CCR5 N-terminal dependence, we determined the sensitivity of each variant to anti-CCR5 N-terminal mAb, CTC-5. All passaged variants were completely resistant to CTC-5; however, the MVC-selected variant became sensitive to CTC-5 when MVC (1 μM) was added in the assay, as reported previously (Berro *et al.*, 2009). These results suggest that the four mutations associated with the CCR5-binding site in the MVC-selected variant might create an increased dependency on interaction with the CCR5 N terminus.

In this study, we attempted to determine the difference between the MVC-selected and low-CCR5-adapted variants in parallel using an *in vitro* passage system. Under low concentrations of MVC, the MPI reduction was not observed in either the MVC-selected variant or the low-CCR5-adapted variant, although both passaged variants had common substitutions in the V1, V3 and V5 regions from quasi-species. Compared with the baseline viruses, under high concentrations of MVC, the resistant variants acquired mutations within the area of the CCR5-binding site in gp120 by evolution and/or selection from minor subsets. Following acquisition of the latter mutations, the variants with mutant Env showed a considerably reduced MPI (24 %). These results indicate that mutants arising from passage in low-CCR5-expressing cells can influence the IC_{50} shift, but not a reduction in the MPI.

One previous study showed that although numerous changes were observed in V3 and other regions of gp160, genotypic analysis of the cloned *env* sequences revealed no specific mutational pattern associated with reduced susceptibility to VCV in a phase 2 clinical trial (Pantophlet & Burton, 2006). Using the Los Alamos Database, we found that the frequencies of the four mutations occurred in <10 % of 1501 subtype B viruses (V200I, 5.1 %; T297I, 5.9 %; K305R, 9.5 %; M434I, 2.5 %). Assays for these mutations might provide useful clinical markers for determining the sensitivity of HIV-1 to MVC. One limitation of the present study was that only one primary isolate was used and a single *in vitro* passage series was used for variant selection. Further studies using multiple isolates and multiple passage cultures are required to determine if this MVC-susceptibility model applies to other HIV subtypes and cell systems. Ogert *et al.* (2009) and Anastassopoulou *et al.* (2009) reported that multistep resistance mutations during *in vitro* selection that reduced the MPI values to VCV were driven by the K305R substitution and the H308P substitution was related to a reduction in the MPI plateau level to VCV resistance. Henrich *et al.* (2010) also reported such mutations *in vivo*, as S306P was not detected in the baseline virus population, but was necessary for maximal resistance when incorporated into V3 backbones that included pre-existing VCV resistance mutations. Our *in vitro* study also showed that the K305R mutation contributed to maximal resistance to MVC when incorporated into V3 and CCR5 N-terminal-binding site backbones that included pre-existing MVC resistance mutations. Moreover, our MVC-selected variant with MVC (1 μM) became sensitive to the CCR5 N-terminal mAb (data not shown). Conversely, Roche *et al.* (2011a) reported that the MVC-resistant variants increased reliance on sulfated tyrosine residues in the CCR5 N terminus without common gp120 resistance mutations. One resistant clone (17-Res) harboured I317F, A322D and I323V substitutions in the V3 loop, whilst the other resistant clone (24-Res) had P308S and Ala inserted at the 313 position in the V3. In our MVC-resistant variant, we found some mutations at the same positions (305, 309, 317 and 321) in the V3 region as those of 17-Res and 24-Res clones (Roche *et al.*, 2011a). It is still not clear whether such mutations around the V3 loop stem region contribute to increased reliance on the CCR5 N terminus, and further studies are needed to determine the relationship between each mutation and CCR5 N terminus dependency.

HIV Env evades antibody recognition of conserved epitopes by several means, including decoration with a dense glycan shield, hypervariable loops that mask conserved features and high intrinsic conformational dynamics that render it a poorly defined antigen (Pantophlet & Burton, 2006). In the present study, the infectious clone with the Env of the low-CCR5-adapted virus became sensitive to anti-CD4i mAb, but not anti-V3 mAb and autologous plasma IgGs. Conversely, the clone with the highly MVC-resistant Env was neutralized by the anti-V3 mAb at low concentrations (<0.1 μg ml^{-1}) and also by the autologous plasma IgGs. These findings suggest that the low-CCR5-adapted mutations are related to accessibility of the anti-CD4i mAb to its epitopes, whilst the greater number of mutations in the MVC-selected virus may provide access to the epitopes of

not only anti-CD4bs and anti-CD4i mAbs, but also the anti-V3 mAb and autologous plasma IgGs. In preliminary data, we have confirmed the presence of such anti-CD4i and anti-V3 antibodies in plasma samples from the subject from whom HIV-1_{KP-5} was isolated (unpublished data). *In vivo*, where potent levels of Env neutralizing antibodies may be present, the MVC-selected variants may become neutralization-sensitive and not survive. For this reason, it is possible that CCR5 inhibitors, such as MVC, suppress HIV replication for long periods, especially in patients with high levels of circulating anti-Env neutralizing antibodies prior to treatment with MVC.

As some of the mutations in the MVC-selected variant are close to the epitope for KD-247, those mutations might influence the sensitivity and/or binding affinity to KD-247. Moreover, the mutations around and within the V3 loop may also affect the association with the V2 loop by opening of the trimer. Our study did not allow us to distinguish this possibility. Thus, further studies with single and combinations of mutations in Env to determine the binding affinity to the neutralizing antibodies by FACS and/or ELISA are ongoing.

Following CD4 binding, the CD4-binding site on gp120 becomes ordered and the bridging sheet subdomain forms, drawing the V1/V2 loops into a 'down' orientation and positioning them alongside CD4 (Guttman *et al.*, 2012). The MVC-selected variant in our study became highly sensitive to anti-CD4i and V3 neutralizing mAbs compared with the passage control virus. Further analysis of the effect of the CCR5 inhibitor-resistant Env to neutralizing antibodies would be of interest because, as reported in our previous work (Yoshimura *et al.*, 2006), the anti-V3 mAb KD-247-resistant variant became highly sensitive to CCR5 inhibitors.

METHODS

Viruses. Primary HIV-1 viruses were isolated from patients and passaged in PHA-activated PBMCs. Infected PBMCs were co-cultured for 5 days with PM1/CCR5 cells and the culture supernatants were stored at −150 °C until use (Yoshimura *et al.*, 2010). HIV-1_{KP-5} was isolated from a subject prior to MVC therapy but who has subsequently been taking combination antiretroviral therapy containing MVC since September 2009. The HIV-1_{KP-5} was isolated before starting the combination antiretroviral therapy.

Cells, culture conditions and reagents. The $CD4^+$ T-cell line PM1 (Lusso *et al.*, 1995) was obtained through the AIDS Research and Reference Reagent Program (ARRRP). The PM1/CCR5 cell line was a kind gift from Dr Yosuke Maeda (Kumamoto University, Kumamoto, Japan) (Maeda *et al.*, 2008b). The CCR5 inhibitor MVC was kindly provided by Pfizer (Groton, CT, USA).

Flow cytometric analysis. PM1 and PM1/CCR5 cells were analysed for surface expression of CCR5 and CXCR4. The cells (5×10^5) were incubated with phycoerythrin-labelled anti-CCR5 mAb 2D7, phycoerythrin-labelled anti-CXCR4 mAb 12G5 or isotype-matched control mAbs (BD Biosciences) and analysed using a FACSCalibur (Becton Dickinson).

***In vitro* selection of HIV-1 variants using anti-HIV drugs.** HIV-1_{KP-5} was infected into PM1/CCR5 cells and treated with various concentrations of MVC to induce the production of MVC-resistant variants as described previously (Harada *et al.*, 2013; Hatada *et al.*, 2010; Yoshimura *et al.*, 2006, 2010), with minor modifications. Briefly, PM1/CCR5 cells (4×10^4) were exposed to 500 $TCID_{50}$ HIV-1_{KP-5} and cultured in the presence of MVC. The culture supernatant was harvested on day 7 and used to infect fresh PM1/CCR5 cells for the next round of culture in the presence of increasing concentrations of MVC. We also passaged the virus in the absence of MVC in PM1/CCR5 cells and the parental cell line PM1. Proviral DNA was extracted from lysates of infected cells at different passages and subjected to nucleotide sequencing.

Amplification of proviral DNA and nucleotide sequencing. Proviral DNA was subjected to PCR amplification using PrimeSTAR GXL DNA polymerase and Ex-*Taq* polymerase (Takara) as described previously (Harada *et al.*, 2013; Hatada *et al.*, 2010; Yoshimura *et al.*, 2006, 2010). Primers 1B and H were used for the gp120 region (Harada *et al.*, 2013; Hatada *et al.*, 2010). The first-round PCR products were used directly in a second round of PCR using primers 2B and F for gp120 (Harada *et al.*, 2013; Hatada *et al.*, 2010). The second-round PCR products were purified and cloned into the pGEM-T Easy Vector (Promega), and the *env* region in each passaged virus was sequenced using a 3500xL Genetic Analyzer (Applied Biosystems).

Susceptibility assay. The sensitivities of the passaged viruses to various drugs were determined as described previously (Harada *et al.*, 2013; Hatada *et al.*, 2010; Yoshimura *et al.*, 2006, 2010), with minor modifications. Briefly, PM1/CCR5 cells were plated in 96-well round-bottom plates (2×10^3 cells per well), exposed to 100 $TCID_{50}$ of the viruses in the presence of various concentrations of drugs and incubated at 37 °C for 7 days. The IC_{50} values were then determined using a Cell Counting kit-8 (WST-8 assay; Dojindo Laboratories). All assays were performed in duplicate or triplicate.

PHA-activated PBMCs (1×10^6 cells ml^{-1}) were exposed to 100 $TCID_{50}$ of each HIV-1 strain and cultured in the presence or absence of various concentrations of drugs in 96-well microculture plates. The concentration of p24 antigen produced by the cells was determined on day 7 using a Lumipulse F system (Fujirebio) (Maeda *et al.*, 2001). IC_{50} values were determined by comparison with the p24 production level in drug-free control cell cultures (Shirasaka *et al.*, 1995). All assays were performed in triplicate.

Construction of chimeric NL4-3/KP-5 *env* proviruses. Chimeric proviruses were constructed from the pNL4-3 proviral plasmid (ARRRP) by overlapping PCR as described previously (Shibata *et al.*, 2007), with minor modifications. Briefly, the gp160 coding sequences were amplified from the cloning vectors using the primers EnvFv (5′-AGCAGAAGACAGTGGCAATGAGAGCGAAG-3′) and EnvR (5′-TTTTGACCACTTGCCACCCATCTTATAGC-3′). A portion of the NL4-3 provirus spanning nt 5284–6232 was amplified with primers NL(5284)F (5′-GGTCAGGGAGTCTCCATAGAATGGAGG-3′) and NL(6232)Rv (5′-CTTCGCTCTCATTGCCACTGTCTTCTGCT-3′). This fragment encompasses the unique *Eco*RI restriction site in pNL4-3. Another fragment from the NL4-3 provirus spanning nt 8779–9045 was amplified using the primers NL(8779)F (5-GCTATAAGATGGGTGGCAAGTGGTCAAAA-3) and NL(9045)R (5-GATCTACAGCTGCCTTGTAAGTCATTGGTC-3). This fragment includes the unique *Xho*I restriction site in pNL4-3. Overlapping PCR was used to join the gp160 coding sequence from the desired clone to the fragment encompassing nt 8779–9045 that had been amplified from pNL4-3. The resulting fragment was then similarly joined to the amplified fragment encompassing nt 5284–6232 from pNL4-3.

The sensitivities of the three infectious clones to KD-247 (anti-V3 mAb) (Eda *et al.*, 2006), b12 (anti-CD4bs mAb; kindly provided by

Dr Dennis Burton, Scripps Research Institute, La Jolla, CA) (Kessler *et al.*, 1997), 4E9C (anti-CD4i mAb) (Yoshimura *et al.*, 2010) and autologous plasma IgGs were also determined by the WST-8 assay. Plasma samples were collected from the patient seven times from January 2010 to April 2011 and purified using Protein A Sepharose Fast Flow (GE Healthcare) (Kimura *et al.*, 2002; Yoshimura *et al.*, 2010). The purified plasma IgGs were designated KP-5-IgG-1 to KP-5-IgG-7.

Crystal structure of gp120. To compare the sequences of the MVC-selected and low-CCR5-adapted variants in 3D space, the crystal structures of the gp120 monomer and trimer were obtained from the PDB (IDs: 2B4C and 3J5M). Figures were generated using ViewerLite version 5.0 (Accelrys).

ACKNOWLEDGEMENTS

We thank The Chemo-Sero-Therapeutic Research Institute for kindly providing mAb KD-247. We also thank Dr Dennis Burton for kindly providing mAb b12. We are grateful to Dr Yosuke Maeda for providing the PM1/CCR5 cells. We also thank Aki Yamaguchi, Akiko Honda-Shibata and Noriko Shirai for excellent technical assistance. We greatly thank Dr Mark de Souza for his English proofreading. This work was supported in part by the Ministry of Health, Labour and Welfare of Japan (H22-RPEDMD-G-007 to S. M. and K. Y.; H23-AIDS-G-001, H24-AIDS-G-006 and H25-G-006 to K. Y.), the Ministry of Education, Culture, Sports, Science and Technology of Japan (24591485 and 23590548 to K. Y.; 24590199 to S. H.), and the Cooperative Research Project on Clinical and Epidemiological Studies of Emerging and Re-emerging Infectious Diseases and the Global COE Program (Global Education and Research Centre Aiming at the Control of AIDS), MEXT, Japan.

REFERENCES

Anastassopoulou, C. G., Ketas, T. J., Klasse, P. J. & Moore, J. P. (2009). Resistance to CCR5 inhibitors caused by sequence changes in the fusion peptide of HIV-1 gp41. *Proc Natl Acad Sci U S A* **106**, 5318–5323.

Berger, E. A., Murphy, P. M. & Farber, J. M. (1999). Chemokine receptors as HIV-1 coreceptors: roles in viral entry, tropism, and disease. *Annu Rev Immunol* **17**, 657–700.

Berro, R., Sanders, R. W., Lu, M., Klasse, P. J. & Moore, J. P. (2009). Two HIV-1 variants resistant to small molecule CCR5 inhibitors differ in how they use CCR5 for entry. *PLoS Pathog* **5**, e1000548.

Brelot, A., Heveker, N., Adema, K., Hosie, M. J., Willett, B. & Alizon, M. (1999). Effect of mutations in the second extracellular loop of CXCR4 on its utilization by human and feline immunodeficiency viruses. *J Virol* **73**, 2576–2586.

Cormier, E. G. & Dragic, T. (2002). The crown and stem of the V3 loop play distinct roles in human immunodeficiency virus type 1 envelope glycoprotein interactions with the CCR5 coreceptor. *J Virol* **76**, 8953–8957.

Dorr, P., Westby, M., Dobbs, S., Griffin, P., Irvine, B., Macartney, M., Mori, J., Rickett, G., Smith-Burchnell, C. & other authors (2005). Maraviroc (UK-427,857), a potent, orally bioavailable, and selective small-molecule inhibitor of chemokine receptor CCR5 with broad-spectrum anti-human immunodeficiency virus type 1 activity. *Antimicrob Agents Chemother* **49**, 4721–4732.

Dragic, T., Trkola, A., Thompson, D. A., Cormier, E. G., Kajumo, F. A., Maxwell, E., Lin, S. W., Ying, W., Smith, S. O. & other authors (2000). A binding pocket for a small molecule inhibitor of HIV-1 entry within the transmembrane helices of CCR5. *Proc Natl Acad Sci U S A* **97**, 5639–5644.

Eda, Y., Takizawa, M., Murakami, T., Maeda, H., Kimachi, K., Yonemura, H., Koyanagi, S., Shiosaki, K., Higuchi, H. & other authors (2006). Sequential immunization with V3 peptides from primary human immunodeficiency virus type 1 produces cross-neutralizing antibodies against primary isolates with a matching narrow-neutralization sequence motif. *J Virol* **80**, 5552–5562.

Farzan, M., Mirzabekov, T., Kolchinsky, P., Wyatt, R., Cayabyab, M., Gerard, N. P., Gerard, C., Sodroski, J. & Choe, H. (1999). Tyrosine sulfation of the amino terminus of CCR5 facilitates HIV-1 entry. *Cell* **96**, 667–676.

Fätkenheuer, G., Nelson, M., Lazzarin, A., Konourina, I., Hoepelman, A. I., Lampiris, H., Hirschel, B., Tebas, P., Raffi, F. & other authors (2008). Subgroup analyses of maraviroc in previously treated R5 HIV-1 infection. *N Engl J Med* **359**, 1442–1455.

Gulick, R. M., Lalezari, J., Goodrich, J., Clumeck, N., DeJesus, E., Horban, A., Nadler, J., Clotet, B., Karlsson, A. & other authors (2008). Maraviroc for previously treated patients with R5 HIV-1 infection. *N Engl J Med* **359**, 1429–1441.

Guttman, M., Kahn, M., Garcia, N. K., Hu, S. L. & Lee, K. K. (2012). Solution structure, conformational dynamics, and CD4-induced activation in full-length, glycosylated, monomeric HIV gp120. *J Virol* **86**, 8750–8764.

Harada, S., Yoshimura, K., Yamaguchi, A., Boonchawalit, S., Yusa, K. & Matsushita, S. (2013). Impact of antiretroviral pressure on selection of primary human immunodeficiency virus type 1 envelope sequences *in vitro*. *J Gen Virol* **94**, 933–943.

Hatada, M., Yoshimura, K., Harada, S., Kawanami, Y., Shibata, J. & Matsushita, S. (2010). Human immunodeficiency virus type 1 evasion of a neutralizing anti-V3 antibody involves acquisition of a potential glycosylation site in V2. *J Gen Virol* **91**, 1335–1345.

Henrich, T. J., Tsibris, A. M., Lewine, N. R., Konstantinidis, I., Leopold, K. E., Sagar, M. & Kuritzkes, D. R. (2010). Evolution of CCR5 Antagonist Resistance in an HIV-1 Subtype C Clinical Isolate. *J Acquir Immune Defic Syndr* **55**, 420–427.

Huang, C. C., Tang, M., Zhang, M. Y., Majeed, S., Montabana, E., Stanfield, R. L., Dimitrov, D. S., Korber, B., Sodroski, J. & other authors (2005). Structure of a V3-containing HIV-1 gp120 core. *Science* **310**, 1025–1028.

Kessler, J. A., II, McKenna, P. M., Emini, E. A., Chan, C. P., Patel, M. D., Gupta, S. K., Mark, G. E., III, Barbas, C. F., III, Burton, D. R. & Conley, A. J. (1997). Recombinant human monoclonal antibody IgG1b12 neutralizes diverse human immunodeficiency virus type 1 primary isolates. *AIDS Res Hum Retroviruses* **13**, 575–582.

Kimura, T., Yoshimura, K., Nishihara, K., Maeda, Y., Matsumi, S., Koito, A. & Matsushita, S. (2002). Reconstitution of spontaneous neutralizing antibody response against autologous human immunodeficiency virus during highly active antiretroviral therapy. *J Infect Dis* **185**, 53–60.

Kuhmann, S. E., Pugach, P., Kunstman, K. J., Taylor, J., Stanfield, R. L., Snyder, A., Strizki, J. M., Riley, J., Baroudy, B. M. & other authors (2004). Genetic and phenotypic analyses of human immunodeficiency virus type 1 escape from a small-molecule CCR5 inhibitor. *J Virol* **78**, 2790–2807.

Landovitz, R. J., Angel, J. B., Hoffmann, C., Horst, H., Opravil, M., Long, J., Greaves, W. & Fätkenheuer, G. (2008). Phase II study of vicriviroc versus efavirenz (both with zidovudine/lamivudine) in treatment-naive subjects with HIV-1 infection. *J Infect Dis* **198**, 1113–1122.

Lusso, P., Cocchi, F., Balotta, C., Markham, P. D., Louie, A., Farci, P., Pal, R., Gallo, R. C. & Reitz, M. S., Jr (1995). Growth of macrophage-tropic and primary human immunodeficiency virus type 1 (HIV-1)

isolates in a unique CD4$^+$ T-cell clone (PM1): failure to down-regulate CD4 and to interfere with cell-line-tropic HIV-1. *J Virol* **69**, 3712–3720.

Lyumkis, D., Julien, J. P., de Val, N., Cupo, A., Potter, C. S., Klasse, P. J., Burton, D. R., Sanders, R. W., Moore, J. P. & other authors (2013). Cryo-EM structure of a fully glycosylated soluble cleaved HIV-1 envelope trimer. *Science* **342**, 1484–1490.

Maeda, K., Yoshimura, K., Shibayama, S., Habashita, H., Tada, H., Sagawa, K., Miyakawa, T., Aoki, M., Fukushima, D. & Mitsuya, H. (2001). Novel low molecular weight spirodiketopiperazine derivatives potently inhibit R5 HIV-1 infection through their antagonistic effects on CCR5. *J Biol Chem* **276**, 35194–35200.

Maeda, K., Das, D., Ogata-Aoki, H., Nakata, H., Miyakawa, T., Tojo, Y., Norman, R., Takaoka, Y., Ding, J. & other authors (2006). Structural and molecular interactions of CCR5 inhibitors with CCR5. *J Biol Chem* **281**, 12688–12698.

Maeda, K., Das, D., Yin, P. D., Tsuchiya, K., Ogata-Aoki, H., Nakata, H., Norman, R. B., Hackney, L. A., Takaoka, Y. & Mitsuya, H. (2008a). Involvement of the second extracellular loop and transmembrane residues of CCR5 in inhibitor binding and HIV-1 fusion: insights into the mechanism of allosteric inhibition. *J Mol Biol* **381**, 956–974.

Maeda, Y., Yusa, K. & Harada, S. (2008b). Altered sensitivity of an R5X4 HIV-1 strain 89.6 to coreceptor inhibitors by a single amino acid substitution in the V3 region of gp120. *Antiviral Res* **77**, 128–135.

Marozsan, A. J., Kuhmann, S. E., Morgan, T., Herrera, C., Rivera-Troche, E., Xu, S., Baroudy, B. M., Strizki, J. & Moore, J. P. (2005). Generation and properties of a human immunodeficiency virus type 1 isolate resistant to the small molecule CCR5 inhibitor, SCH-417690 (SCH-D). *Virology* **338**, 182–199.

Ogert, R. A., Wojcik, L., Buontempo, C., Ba, L., Buontempo, P., Ralston, R., Strizki, J. & Howe, J. A. (2008). Mapping resistance to the CCR5 co-receptor antagonist vicriviroc using heterologous chimeric HIV-1 envelope genes reveals key determinants in the C2-V5 domain of gp120. *Virology* **373**, 387–399.

Ogert, R. A., Ba, L., Hou, Y., Buontempo, C., Qiu, P., Duca, J., Murgolo, N., Buontempo, P., Ralston, R. & Howe, J. A. (2009). Structure–function analysis of human immunodeficiency virus type 1 gp120 amino acid mutations associated with resistance to the CCR5 coreceptor antagonist vicriviroc. *J Virol* **83**, 12151–12163.

Ogert, R. A., Hou, Y., Ba, L., Wojcik, L., Qiu, P., Murgolo, N., Duca, J., Dunkle, L. M., Ralston, R. & Howe, J. A. (2010). Clinical resistance to vicriviroc through adaptive V3 loop mutations in HIV-1 subtype D gp120 that alter interactions with the N-terminus and ECL2 of CCR5. *Virology* **400**, 145–155.

Pantophlet, R. & Burton, D. R. (2006). GP120: target for neutralizing HIV-1 antibodies. *Annu Rev Immunol* **24**, 739–769.

Pugach, P., Marozsan, A. J., Ketas, T. J., Landes, E. L., Moore, J. P. & Kuhmann, S. E. (2007). HIV-1 clones resistant to a small molecule CCR5 inhibitor use the inhibitor-bound form of CCR5 for entry. *Virology* **361**, 212–228.

Ratcliff, A. N., Shi, W. & Arts, E. J. (2013). HIV-1 resistance to maraviroc conferred by a CD4 binding site mutation in the envelope glycoprotein gp120. *J Virol* **87**, 923–934.

Roche, M., Jakobsen, M. R., Ellett, A., Salimiseyedabad, H., Jubb, B., Westby, M., Lee, B., Lewin, S. R., Churchill, M. J. & Gorry, P. R. (2011a). HIV-1 predisposed to acquiring resistance to maraviroc (MVC) and other CCR5 antagonists *in vitro* has an inherent, low-level ability to utilize MVC-bound CCR5 for entry. *Retrovirology* **8**, 89.

Roche, M., Jakobsen, M. R., Sterjovski, J., Ellett, A., Posta, F., Lee, B., Jubb, B., Westby, M., Lewin, S. R. & other authors (2011b). HIV-1 escape from the CCR5 antagonist maraviroc associated with an altered and less-efficient mechanism of gp120–CCR5 engagement that attenuates macrophage tropism. *J Virol* **85**, 4330–4342.

Shibata, J., Yoshimura, K., Honda, A., Koito, A., Murakami, T. & Matsushita, S. (2007). Impact of V2 mutations on escape from a potent neutralizing anti-V3 monoclonal antibody during *in vitro* selection of a primary human immunodeficiency virus type 1 isolate. *J Virol* **81**, 3757–3768.

Shirasaka, T., Kavlick, M. F., Ueno, T., Gao, W. Y., Kojima, E., Alcaide, M. L., Chokekijchai, S., Roy, B. M., Arnold, E. & Yarchoan, R. (1995). Emergence of human immunodeficiency virus type 1 variants with resistance to multiple dideoxynucleosides in patients receiving therapy with dideoxynucleosides. *Proc Natl Acad Sci U S A* **92**, 2398–2402.

Tilton, J. C., Wilen, C. B., Didigu, C. A., Sinha, R., Harrison, J. E., Agrawal-Gamse, C., Henning, E. A., Bushman, F. D., Martin, J. N. & other authors (2010). A maraviroc-resistant HIV-1 with narrow cross-resistance to other CCR5 antagonists depends on both N-terminal and extracellular loop domains of drug-bound CCR5. *J Virol* **84**, 10863–10876.

Tsamis, F., Gavrilov, S., Kajumo, F., Seibert, C., Kuhmann, S., Ketas, T., Trkola, A., Palani, A., Clader, J. W. & other authors (2003). Analysis of the mechanism by which the small-molecule CCR5 antagonists SCH-351125 and SCH-350581 inhibit human immunodeficiency virus type 1 entry. *J Virol* **77**, 5201–5208.

Tsibris, A. M., Sagar, M., Gulick, R. M., Su, Z., Hughes, M., Greaves, W., Subramanian, M., Flexner, C., Giguel, F. & other authors (2008). *In vivo* emergence of vicriviroc resistance in a human immunodeficiency virus type 1 subtype C-infected subject. *J Virol* **82**, 8210–8214.

Westby, M., Lewis, M., Whitcomb, J., Youle, M., Pozniak, A. L., James, I. T., Jenkins, T. M., Perros, M. & van der Ryst, E. (2006). Emergence of CXCR4-using human immunodeficiency virus type 1 (HIV-1) variants in a minority of HIV-1-infected patients following treatment with the CCR5 antagonist maraviroc is from a pretreatment CXCR4-using virus reservoir. *J Virol* **80**, 4909–4920.

Westby, M., Smith-Burchnell, C., Mori, J., Lewis, M., Mosley, M., Stockdale, M., Dorr, P., Ciaramella, G. & Perros, M. (2007). Reduced maximal inhibition in phenotypic susceptibility assays indicates that viral strains resistant to the CCR5 antagonist maraviroc utilize inhibitor-bound receptor for entry. *J Virol* **81**, 2359–2371.

Wyatt, R. & Sodroski, J. (1998). The HIV-1 envelope glycoproteins: fusogens, antigens, and immunogens. *Science* **280**, 1884–1888.

Yoshimura, K., Shibata, J., Kimura, T., Honda, A., Maeda, Y., Koito, A., Murakami, T., Mitsuya, H. & Matsushita, S. (2006). Resistance profile of a neutralizing anti-HIV monoclonal antibody, KD-247, that shows favourable synergism with anti-CCR5 inhibitors. *AIDS* **20**, 2065–2073.

Yoshimura, K., Harada, S., Shibata, J., Hatada, M., Yamada, Y., Ochiai, C., Tamamura, H. & Matsushita, S. (2010). Enhanced exposure of human immunodeficiency virus type 1 primary isolate neutralization epitopes through binding of CD4 mimetic compounds. *J Virol* **84**, 7558–7568.

Yuan, Y., Maeda, Y., Terasawa, H., Monde, K., Harada, S. & Yusa, K. (2011). A combination of polymorphic mutations in V3 loop of HIV-1 gp120 can confer noncompetitive resistance to maraviroc. *Virology* **413**, 293–299.

Yusa, K., Maeda, Y., Fujioka, A., Monde, K. & Harada, S. (2005). Isolation of TAK-779-resistant HIV-1 from an R5 HIV-1 GP120 V3 loop library. *J Biol Chem* **280**, 30083–30090.

Screening for Protein Kinase C Ligands Using Fluorescence Resonance Energy Transfer

Nami Ohashi, Wataru Nomura,* Natsuki Minato, and Hirokazu Tamamura*

Department of Medicinal Chemistry, Institute of Biomaterials and Bioengineering, Tokyo Medical and Dental University; 2–3–10 Kandasurugadai, Chiyoda-ku, Tokyo 101–0062, Japan.
Received June 3, 2014; accepted July 30, 2014; advance publication released online August 8, 2014

Protein kinase C (PKC) is correlated with cell signaling pathways and also receives attention as a therapeutic target for cancer and Alzheimer-type dementia. The application of Förster/fluorescence resonance energy transfer (FRET) phenomena to detect binding between proteins and small molecules, for example, PKC and its ligands, underlies a fluorescence-based assay method suitable for high-throughput screening. To accelerate studies on PKC functions in processing signals using small molecules and the development of drugs that target PKC, novel methods for the assessment of the PKC binding affinity of compounds are necessary. We previously developed solvatochromic fluorophore-based methods for that assessment. In this study, a novel method for a FRET-based PKC binding assay was developed and is expected to overcome the limitations of solvatochromic fluorophores.

Key words protein kinase C; protein kinase C ligand; ligand screening; Förster resonance energy transfer; fluorescence resonance energy transfer

Förster/fluorescence resonance energy transfer (FRET) is the transfer of excitation energy from a fluorescence donor to an acceptor. FRET efficiency and sensitivity depend on the distance between the donor and the acceptor. The FRET phenomenon can be applied as a spectroscopic measure and a probe of conformational change of macro-biomolecules[1–3] and a FRET-mediated competitive assay can be used for studies of the binding between two molecules.[4,5] Radioisotope-based methods are extremely sensitive and are widely used for ligand binding assays, but fluorescent-based assays, which are suitable for high-throughput screening are free of hazards associated with radioactivity. Previously, we described fluorescence-based ligand screening assays as an alternative to radioisotope assays.[6,7]

Protein kinase C (PKC) isozymes, which are classified as Ser/Thr kinases, play a critical role in cellular signaling pathways related to proliferation,[8,9] differentiation,[10] and apoptosis.[11,12] PKC has 11 isozymes which are classified into three subtypes: conventional PKC (cPKC; α, $\beta_{I/II}$, γ), novel PKC (nPKC; δ, ε, η, τ) and atypical PKC (aPKC; ζ, λ, ι). The binding of diacylglycerols (DAG) to the C1 domain of PKC is an important step in an activation process except in the case of aPKC which contains an atypical C1 domain which fails to bind to DAG.[13] Various synthetic PKC ligands targeting the C1 domain have been developed as chemical probes or drug candidates by radioisotope assays.[14–17] We have previously developed a fluorescent assay for PKC-ligand binding affinity using a synthetic PKC δC1b domain labeled with a solvatochromic fluorophore on the edge of its ligand-binding pocket. This can detect ligand binding through changes in the surrounding environment.[18] However, this method would not be suitable for high-throughput screening. The reason might be due to several possibilities: For instance, the change of fluorescence intensity is affected by properties of test compounds. It would be concerned that a fluorescent-dye labeled on the edge of δC1b interrupts the correct folding and influences the precisionaccuracy of assay systems. There are some reports which describe the development of FRET-based PKC assays monitoring kinase activity or ligand interaction by recombinant proteins with combination of genetically encoded fluorescent proteins: cyan fluorescent protein (CFP) and yellow fluorescent protein (YFP), or green fluorescent protein 2 (GFP2) and enhanced yellow fluorescent protein (EYFP).[19,20] The detection is derived from fluorescent changes based on conformational changes of the proteins, but on direct ligand binding. These assay systems are based on the interaction between encoded fluorescent proteins, and an assay system based on the interaction between small fluorescent groups has not been reported to date. Thus, the direct assessment of the PKC ligand binding by FRET or a chemical approach for the construction of FRET-based PKC assays using small fluorescent groups is projected. In this report, the chemical synthesis of a δC1b domain or a PKC ligand containing a FRET acceptor fluorescent dye or a FRET donor fluorescent dye, and the direct detection of the PDBu binding to the PKC δC1b domain by FRET phenomena are described (Fig. 1). In the FRET-based PKC assays, it is not necessary that a fluorescent-dye is introduced on the edge of δC1b, thus the structural stability of the fluorescein-labeled δC1b domain might be maintained. Furthermore, the FRET intensity cannot be directly affected by fluorescent properties of test compounds.

Results and Discussion

Design and Synthesis of FRET-Donor and FRET-Acceptor Molecules Diethylaminocoumarin (DEAC) (λ_{ex}=380 nm, λ_{em}=460 nm, in MeOH) and fluorescein (λ_{ex}=497 nm, λ_{em}=521 nm, in buffer pH 7.4) were used in this study as the FRET donor and the FRET acceptor fluorescent dyes, respectively. Based on our previous reports,[7,18] DAG-γ-lactones, whose structure–activity relationships (SAR), have been studied in detail, were adopted as a template for FRET donor molecules (Fig. 2). We have observed that DAG-γ-lactones with fluorescent dyes such as 6-methoxynaphthalene (6MN) derivatives which contain two aromatic rings at the α-alkylidene position (*sn*-2), possess significant binding affinity for the PKC C1b domain. Furthermore, DEAC is more sensitive to

The authors declare no conflict of interest.

*To whom correspondence should be addressed. e-mail: nomura.mr@tmd.ac.jp; tamamura.mr@tmd.ac.jp

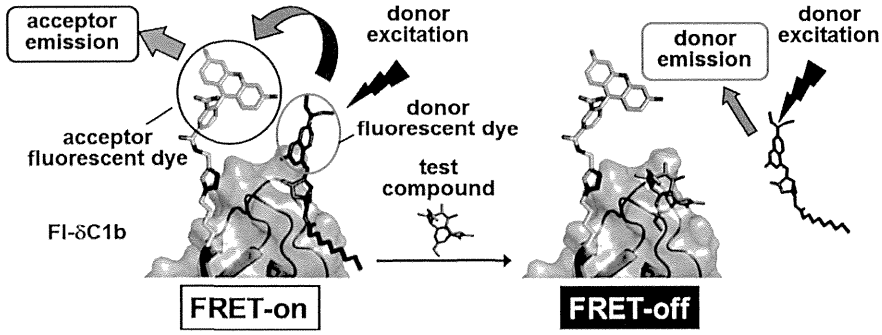

Fig. 1. FRET-Based Competitive Assay of PKC Ligands

In the presence of the Fl-δC1b, the excitation of the donor fluorescent dye (DEAC) causes the fluorescent emission of the acceptor fluorescent dye (fluorescein) (FRET-on). The replacement by a test compound causes the decrease of fluorescence intensity of the acceptor fluorescent dye (FRET-off).

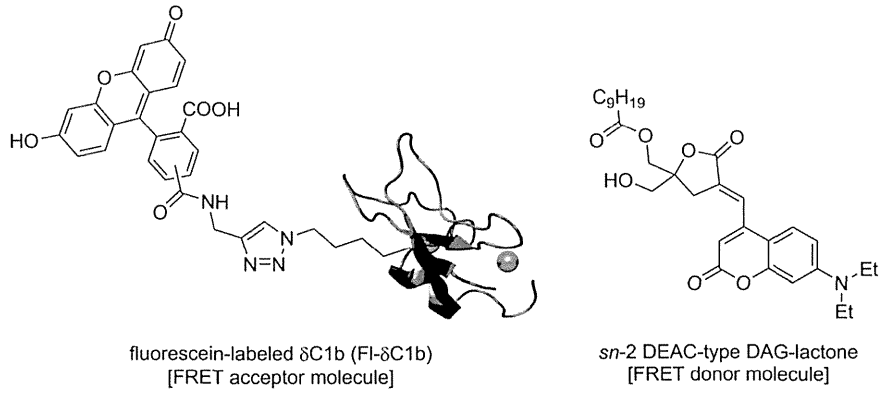

Fig. 2. FRET Donor and FRET Acceptor Molecules

solvents than 6-methoxynaphthalene or dansyl derivatives.[7] In the previous report, a DAG-lactone labeled by DEAC at the acyl position (*sn*-1) showed a 2.6-fold higher K_i value (93.3 nM) than a DAG-lactone labeled by 6MN at the α-alkylidene position (*sn*-2) (35.9 nM). In this study, a DAG-lactone containing DEAC at the α-alkylidene position was designed to improve a K_i value. Initially, a DAG-γ-lactone template was prepared as reported previously.[21] Oxidation of 7-diethylamino-4-methylcoumarin with selenium dioxide gave DEAC possessing an aldehyde group at the C4 position,[22] and this was followed by an aldol condensation with the lactone **3**. Deprotection of *tert*-butyldiphenylsilyl (TBDPS) and finally, monoacylation of the resulting diol gave *sn*-2 DEAC-type DAG-lactone **6** (*E* isomer, racemic) (Chart 1). DAG-γ-lactone derivatives have been used as racemic compounds.[14,23–25]

The C1b domain, residues 231 to 281 of PKCδ, was used as an acceptor molecule. Val235 was selected as the position to be labeled with fluorescein based on the following rationale: Since Val235 is located in the solvent accessible area, it is presumed that the labeled fluorescein would not disturb folding of the C1b domain (PDB ID: 1PTR). The distance of several dozen nanometers between donor and acceptor transforms FRET from a donor fluorescent dye to an acceptor fluorescent dye and consequently, use of the FRET phenomenon does not require introduction of an acceptor fluorescent dye precisely into the edge of the binding pocket.[18] Accordingly, the fluorescein-labeled δC1b domain (Fl-δC1b) **12** was synthesized by Fmoc solid-phase peptide synthesis as follows. Specifically, condensation with Fmoc-Nle(ε-azide)-OH, followed by cycloaddition of alkyne suspending fluorescein to the azide at the ε-position of the Nle residue, and subsequent native chemical ligation generated Fl-δC1b (**12**) (Chart 2).

Evaluation of *sn*-2 DEAC-Type DAG-Lactone and Synthetic δC1b by the Classical RI Assay The wild type of δC1b(231–281) was synthesized as described previously.[26] The K_d value of the synthetic δC1b domain and the K_i value of *sn*-2 DEAC-type DAG-lactone were determined by the poly(ethylene glycol) precipitation assay.[18,27,28] The RI assay showed the Fl-δC1b domain to possess a K_d value comparable to that of the wild-type, whereas the B_{max} value of Fl-δC1b was four-fold smaller than that of the wild-type (Table 1). Such significant decrease of B_{max} indicated the fluorescent moiety could partially impair the efficiency of folding as described previously: The B_{max} value of C1b for the solvatochromic assay is less than one-tenth.[18] In terms of the efficiency of folding, Fl-δC1b is more suitable than C1b for the solvatochromic assay. The *sn*-2 DEAC-type DAG-lactone showed modest affinity for the δC1b domain (K_i=182±18 nM, Table 2). To screen ligand candidates, a competitive probe with high affinity might not be suitable and the *sn*-2 DEAC-type DAG-lactone could be useful for the development of new screening methods.

FRET Experiments When the *sn*-2 DEAC-type DAG-lactone binds to Fl-δC1b, the distance between the donor fluorescent dye (DEAC) and the acceptor fluorescent dye (fluorescein) might be sufficient for energy transfer from the donor to the acceptor (Fig. 1). If a test compound binds to Fl-δC1b competitively, the distance between the donor and the acceptor might be too great to support FRET, and in such a case, the excitation of the donor fluorescence might cause emission of

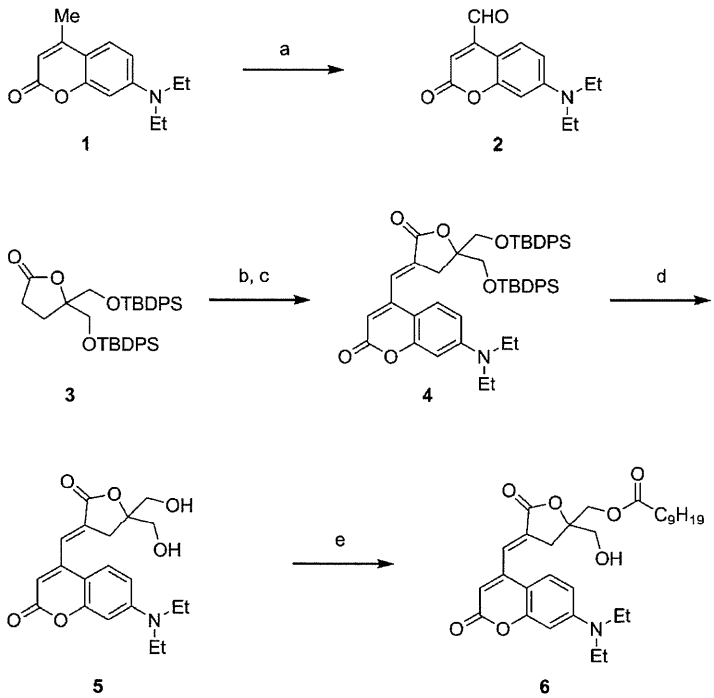

Reagents and conditions: (a) SeO_2, chlorobenzene, reflux; (b) **2**, LDA, THF, −78°C; (c) MsCl, Et_3N, DBU, DCM, 0°C to rt; (d) TBAF, THF; (e) $C_9H_{19}C(O)Cl$, Et_3N, THF.
Chart 1. Synthesis of DEAC-Type DAG-Lactone **6**

the donor fluorescence. In practice, the addition of Fl-δC1b to the assay solution containing *sn*-2 DEAC-type DAG-lactone resulted in an increase of fluorescent intensity of the acceptor (fluorescein). If this was followed by the addition of PDBu as a competitive ligand, a 14% decrease of fluorescent intensity (Figs. 3A–C) was observed. Since the decrease of fluorescent intensity was nearly saturated at 2 μM PDBu, the PDBu titration did not show a concentration-dependent manner (Fig. 3C). In Fig. 3B, the decrease of fluorescent intensity of the donor observed upon the addition of PDBu is due to the influence of solvatochromism of the donor fluorescent dye (DEAC). Since direct excitation of the acceptor was observed upon the titration of Fl-δC1b in the absence of the donor, *sn*-2 DEAC-type DAG-lactone (Fig. 3D), the increase in the acceptor fluorescence failed to reach saturation (Fig. 3A). However, the PDBu titration caused FRET-off, indicating that by use of *sn*-2 DEAC-type DAG-lactone and Fl-δC1b, PKC ligand binding was detected by change of the acceptor fluorescent intensity based on the FRET phenomenon. The IC_{50} values of test compounds can be calculated with the FRET assay in case serial diluted concentrations are used.

Conclusion

In this study, a FRET-based competitive assay has been developed. *sn*-2 DEAC-type DAG-lactone as a donor molecule and Fl-δC1b as an accepter molecule were synthesized and it was confirmed that the *sn*-2 DEAC-type DAG-lactone probe possesses modest affinity for the δC1b domain and Fl-δC1b for the [^{3}H]PDBu binding affinity. The addition of PDBu to the mixture of *sn*-2 DEAC-type DAG-lactone and Fl-δC1b caused a decrease of the acceptor fluorescent intensity upon the irradiation with the donor's excitation wavelength. The FRET-based competitive assay could be useful for PKC ligand screening and applicable to other protein-small molecule interactions.

Experimental

General For thin-layer chromatography (TLC), Merck 60F254 precoated silica gel plates were employed. Column chromatography was performed with Wakogel C-200 (Wako Pure Chemical Industries, Ltd.) and silica gel 60N (Kanto Chemical Co., Inc.). ^{1}H-NMR (400 MHz) spectra were recorded using a Bruker Avance III 400 spectrometer and ^{1}H-NMR (500 MHz) and ^{13}C-NMR (125 MHz) spectra were recorded using a Bruker Avance 500 spectrometer. Chemical shifts are reported in δ (ppm) relative to Me_4Si (in $CDCl_3$) as the internal standard. Low- and high-resolution mass spectra were recorded on a Bruker Daltonics micrOTOF-2focus. For RP-HPLC, Cosmosil 5C_{18} AR-II column (4.6×250 mm for analytical runs, 20×250 mm for preparative runs, Nacalai Tesque, Inc., Kyoto, Japan) was employed with a linear gradient of CH_3CN and H_2O containing 0.1% (v/v) trifluoroacetic acid (TFA) at a flow rate of 1 cm^3 min^{-1} on a JASCO PU-2089 plus (JASCO Corporation, Ltd., Tokyo, Japan) for analytical runs or 10 cm^3 min^{-1} on a JASCO PU-2086 plus for preparative runs, and eluted products were detected by UV at 220 nm. UV-Vis absorbance spectra measurements were performed with a JASCO V-650 spectrophotometer. Fluorescent spectra were recorded on a JASCO FP-6600 spectrofluorometer equipped with 1.0 cm path length quartz cuvette.

4-((5,5-Bis(((*tert*-butyldiphenylsilyl)oxy)methyl)-2-oxodihydrofuran-3(2*H*)-ylidene)methyl)-7-(diethylamino)-2*H*-chromen-2-one (4) Lithium diisopropylamide (LDA) (260 μL, 0.52 mmol) was added to a solution of lactone **3** (253 mg, 0.4 mmol) in tetrahydrofuran (THF) (1.5 mL) at −78°C and the resulting mixture was stirred for 2 h at −78°C. Aldehyde **2** (180 mg, 0.73 mmol) in THF (1.5 mL) at −78°C was then added to the mixture. The reaction mixture was stirred and allowed to stand at room temperature for 2 h. The reaction was quenched with saturated aqueous NH_4Cl. The aqueous layer was extracted three times with Et_2O. The

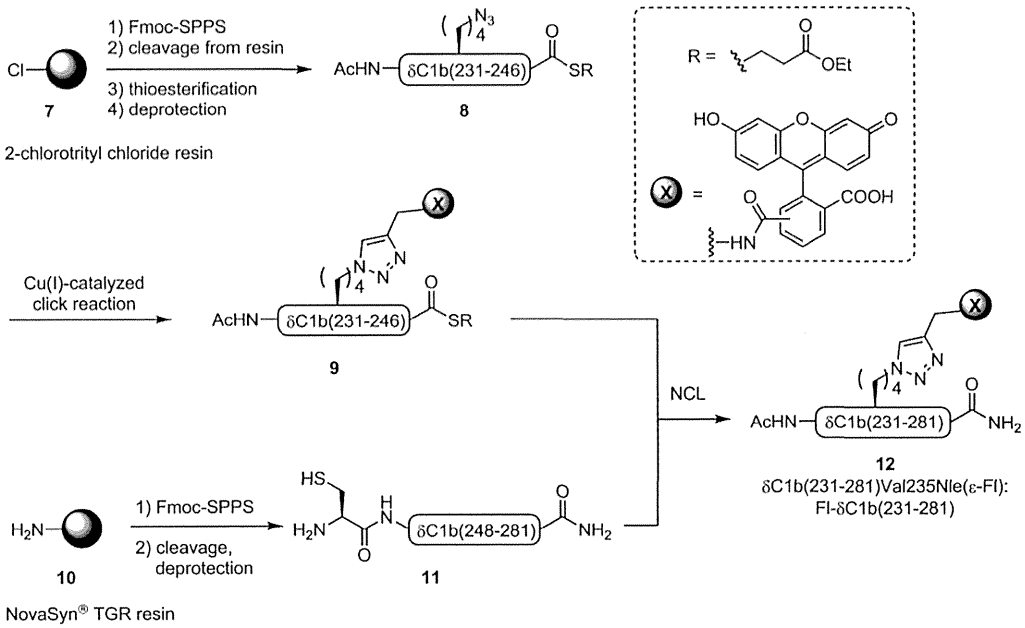

Chart 2. Synthesis of Fluorescein-Labeled δC1b

Table 1. K_d Values of δC1b or Fl-δC1b for [^{3}H]PDBu Binding

Receptor protein	K_d (nM)[a]	B_{max}[b]
δC1b(231–281)	0.41±0.08	100947±6579
Fl-δC1b(231–281)	0.75±0.08	25118±1480

a) Dissociation constant for the synthetic δC1b binding to [^{3}H]PDBu. Mean±S.E.M. *b*) Theoretical maximum receptor occupancy.

Table 2. K_i Values of Fluorescent DAG-Lactone in Specific [^{3}H]PDBu Binding to δC1b

Ligand	K_i (nM)[a]
sn-2 DEAC-type DAG-lactone	182±18
DAG-lactone derivative[b]	6.5±0.8

a) Inhibition constant for the synthetic ligand binding to synthetic δC1b. Mean±S.E.M. *b*) Reference 34.

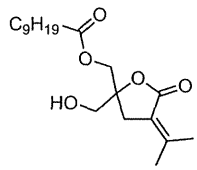

combined organic layer was washed with brine, dried over $MgSO_4$, filtered and concentrated under reduced pressure. To a solution of the crude aldol product in CH_2Cl_2 were added MsCl (62 μL, 0.8 mmol) and Et_3N (223 μL, 1.6 mmol) at 0°C. The resulting mixture was stirred for 2 h then allowed to warm to room temperature. To the reaction mixture was then added 1,8-diazabicyclo[5.4.0]undec-7-ene (DBU) (300 μL, 2.0 mmol) at 0°C, and the resulting mixture was stirred overnight at room temperature. The reaction mixture was concentrated under reduced pressure, followed by purification by silica gel column chromatography (hexane/EtOAc=5 : 1) to give the enone **4** (*E* isomer, 155 mg, 46% yield for two steps) as an orange solid. The *E* isomer was exclusively obtained, which was based on tentative assignment[7,29]: *Rf* 0.43 (hexane/EtOAc=3 : 1); ^{1}H-NMR (400 MHz, $CDCl_3$) δ: 7.43–7.31 (20H, m), 7.20 (1H, d, *J*=9.2 Hz), 6.80 (1H, s), 6.49 (1H, d, *J*=2.4 Hz), 6.29–6.26 (1H, m), 5.91 (1H, s), 3.77 (4H, s), 3.59 (2H, s), 3.35–3.30 (4H, m), 1.16–1.12 (6H, m), 0.94 (18H, s). ^{13}C-NMR (125 MHz, $CDCl_3$) δ: 172.21, 161.81, 156.53, 151.93, 150.69, 135.49, 135.43, 132.85, 132.65, 132.29, 129.91, 127.80, 125.68, 109.15, 108.81, 107.26, 97.63, 89.88, 64.28, 44.63, 28.14, 26.63, 19.14, 12.39. Electrospray ionization-mass spectrometry (ESI-MS) *m/z*: 850.3953 (Calcd for $C_{52}H_{60}NO_6Si_2$ $[M+H]^+$: 850.3954).

4-((5,5-Bis(hydroxymethyl)-2-oxodihydrofuran-3(2*H*)-ylidene)methyl)-7-(diethylamino)-2*H*-chromen-2-one (5) Tetrabutylammonium fluoride (TBAF) (720 μL, 0.72 mmol) was added to a solution of the enone **4** (155 mg, 0.18 mmol) in THF (1 mL) at 0°C. The resulting mixture was stirred for 2 h then allowed to warm to room temperature. The reaction was quenched with H_2O. The aqueous layer was extracted three times with $CHCl_3$. The combined organic layer was washed with brine, dried over $MgSO_4$, filtered and concentrated under reduced pressure. Purification by silica gel column chromatography ($CHCl_3$/MeOH=30 : 1) gave diol **5** (14.7 mg, 63% yield) as an orange solid: *Rf* 0.0 ($CHCl_3$/MeOH=20 : 1); ^{1}H-NMR (400 MHz, $CDCl_3$) δ: 7.31 (1H, d, *J*=8.8 Hz), 7.08 (1H, s), 6.58–6.55 (1H, m), 6.50 (1H, d, *J*=2.4 Hz), 5.99 (1H, s), 3.89–3.80 (4H, m), 3.68 (2H, s), 3.44–3.38 (4H, m), 2.09–2.06 (2H, m), 1.22–1.19 (6H, m). ^{13}C-NMR (125 MHz, $CDCl_3$) δ: 172.30, 162.35, 156.36, 152.07, 150.82, 150.52, 132.48, 125.41, 108.83, 108.59, 107.37, 97.67, 90.11, 63.34, 44.73, 27.67, 12.41. ESI-MS *m/z*: 374.1596 (Calcd for $C_{20}H_{24}NO_6$ $[M+H]^+$: 374.1604).

(4-((7-(Diethylamino)-2-oxo-2*H*-chromen-4-yl)-methylene)-2-(hydroxymethyl)-5-oxotetrahydrofuran-2-yl)-methyl Decanoate (6) Et_3N (20 μL, 0.15 mmol) and decanoyl choride (10 μL, 0.05 mmol) were added to a solution of diol **5** (37 mg, 0.1 mmol) in THF (2 mL) at 0°C. The resulting mixture was stirred for 2 h then allowed to warm to room temperature. The reaction mixture was concentrated under reduced